PHILOSOPHICAL TRANSACTIONS A

rsta.royalsocietypublishing.org

Research

Cite this article: Cawood PA, Hawkesworth CJ, Pisarevsky SA, Dhuime B, Capitanio FA, Nebel O. 2018 Geological archive of the onset of plate tectonics. *Phil. Trans. R. Soc. A* **376**: 20170405.
http://dx.doi.org/10.1098/rsta.2017.0405

Accepted: 21 June 2018

One contribution of 14 to a discussion meeting issue 'Earth dynamics and the development of plate tectonics'.

Subject Areas:
plate tectonics, geochemistry, geology

Keywords:
plate tectonics, Archaean, palaeomagnetics, lithosphere, early Earth

Author for correspondence:
Peter A. Cawood
e-mail: peter.cawood@monash.edu

THE ROYAL SOCIETY PUBLISHING

Geological archive of the onset of plate tectonics

Peter A. Cawood[1,2], Chris J. Hawkesworth[2,3], Sergei A. Pisarevsky[4], Bruno Dhuime[3,5], Fabio A. Capitanio[1] and Oliver Nebel[1]

[1]School of Earth, Atmosphere and Environment, Monash University, Melbourne, VIC 3800, Australia
[2]Department of Earth Sciences, University of St Andrews, St Andrews, Fife KY16 9AL, UK
[3]School of Earth Sciences, University of Bristol, Wills Memorial Building, Queens Road, Bristol BS8 1RJ, UK
[4]ARC Centre of Excellence for Core to Crust Fluid Systems (CCFS) and Earth Dynamics Research Group, The Institute for Geoscience Research (TIGeR), Department of Applied Geology, Curtin University, GPO Box U1987, Perth, WA 6845, Australia
[5]CNRS-UMR 5243, Géosciences Montpellier, Université de Montpellier, Montpellier, France

PAC, 0000-0003-1200-3826; BD, 0000-0002-4146-4739; ON, 0000-0002-5068-7117

Plate tectonics, involving a globally linked system of lateral motion of rigid surface plates, is a characteristic feature of our planet, but estimates of how long it has been the modus operandi of lithospheric formation and interactions range from the Hadean to the Neoproterozoic. In this paper, we review sedimentary, igneous and metamorphic proxies along with palaeomagnetic data to infer both the development of rigid lithospheric plates and their independent relative motion, and conclude that significant changes in Earth behaviour occurred in the mid- to late Archaean, between 3.2 Ga and 2.5 Ga. These data include: sedimentary rock associations inferred to have accumulated in passive continental margin settings, marking the onset of sea-floor spreading; the oldest foreland basin deposits associated with lithospheric convergence; a change from thin, new continental crust of mafic composition to thicker crust of intermediate composition, increased

crustal reworking and the emplacement of potassic and peraluminous granites, indicating stabilization of the lithosphere; replacement of dome and keel structures in granite-greenstone terranes, which relate to vertical tectonics, by linear thrust imbricated belts; the commencement of temporally paired systems of intermediate and high dT/dP gradients, with the former interpreted to represent subduction to collisional settings and the latter representing possible hinterland back-arc settings or ocean plateau environments. Palaeomagnetic data from the Kaapvaal and Pilbara cratons for the interval 2780–2710 Ma and from the Superior, Kaapvaal and Kola-Karelia cratons for 2700–2440 Ma suggest significant relative movements. We consider these changes in the behaviour and character of the lithosphere to be consistent with a gestational transition from a non-plate tectonic mode, arguably with localized subduction, to the onset of sustained plate tectonics.

This article is part of a discussion meeting issue 'Earth dynamics and the development of plate tectonics'.

> If it looks like a duck, swims like a duck, and quacks like a duck, then it probably is a duck (paraphrase of statement by James Riley (1849–1916))

1. Introduction

Plate tectonics is a key feature of our planet. The generation of lithospheric plates and their interactions with mantle, atmosphere and oceans have produced the environment and resources that support the biosphere. Plate tectonics and associated feedbacks are a response to secular cooling of the Earth's interior. But heat loss also occurs through episodic processes such as the emplacement of mantle-derived magma in large igneous provinces (LIP). The relative contribution of, and the control exerted by, continuous and episodic mechanisms of heat loss may have varied through time, perhaps in response to decreasing heat flow (e.g. [1]). This uncertainty has led to debate as to how long plate tectonics has been the modus operandi of lithospheric formation and interaction with suggestions ranging from the Hadean (greater than 4 Ga) to the Neoproterozoic (less than 1 Ga) [2–5]. In significant part, these reflect differences in what might be regarded as the onset of plate tectonics, and how best to recognize plate tectonics in the geological record. A variety of non-plate tectonic modes related to evolving tectonothermal environments have been observed or proposed for other bodies in the solar system and for the early Earth ([6] and references therein). Those advocating a pre-plate tectonic regime for the early Earth generally invoke a fixed or episodically mobile lithosphere, often referred to as a stagnant-lid, but perhaps more appropriately as a single-lid. This is thought to have involved a convecting mantle egressing heat through a combination of conduction, mantle plume-focused igneous activity, and periodic catastrophic overturn of the lithosphere back to the mantle with consequent resurfacing of the solid Earth [7–10].

Uncertainty into the nature and presence of pre-plate tectonic regimes and the timing of any change in tectonic regimes relates to the incompleteness of the rock archive in deep time, differences in the criteria used to infer the existence of plate tectonic and pre-plate tectonic regimes on the early Earth (*ca* greater than 2.5 Ga), and disagreements in the significance and interpretation of available data. It is increasingly accepted, for example, that as subduction may be localized and even transient, evidence for subduction should not necessarily be taken as evidence for sustainable plate tectonics. In this paper, we therefore discuss evidence for the development of rigid lithosphere and for relative lithospheric plate motion derived from proxy data including sedimentary rock associations ascribed to divergent and convergent basin environments, granitoid associations indicative of thickening and stabilization of the lithosphere, structural features indicating a change from vertical to horizontal tectonics, P and T regimes derived from metamorphic rock associations and their tectonic settings, as well as palaeomagnetic data for substantial lateral motion of continental lithosphere blocks. We conclude that significant changes in Earth behaviour occurred in the Meso- to Neoarchaean, around 3.2–2.5 Ga, and that

these changes are consistent with the transition from a pre-plate tectonic, stagnant-lid setting, in which any subduction was transient, to a regime of sustained plate tectonics, involving a linked system of convergent, divergent and strike-slip plate boundaries.

2. Plate tectonics: characteristics

On a plate tectonic Earth, the rigid outer layer, the lithosphere, is broken into tessellated fragments that are in independent horizontal motion about axes of rotation (Euler poles) at a set rate and direction (angular motion). This results in a linked system involving the divergent, convergent and strike-slip relative surface motion of rigid plates (figure 1), with deformation focused at boundary zones. The plates are made up of continental and oceanic lithospheres with contrasting chemical–physical properties [12]. Oceanic lithosphere is thin, dense with low mean elevation (largely submarine), and with new crust of largely mafic composition, whereas continental lithosphere is thicker, less dense, has higher mean elevation, and has a crustal component of more intermediate composition. The area ratio of oceanic to continental lithosphere is approximately 60 : 40 [13], with some 75% of the latter presently exposed above sea level (figure 2). Oceanic lithosphere forms at divergent plate boundaries through adiabatic decompression melting of the asthenosphere, and due to its greater overall density than the underlying asthenosphere, at least for all but the youngest lithosphere, is recycled back into the mantle at convergent plate boundaries [14,15]. The resultant slab pull is the major, on-going driving force of plate tectonics, estimated to contribute some 80% of the overall force, resulting in all oceanic lithosphere younger than 200 Ma. Fluid flux from the subducting oceanic lithosphere results in melting of the overlying mantle wedge and generation of a magmatic arc in the upper plate [16–18]. In contrast with oceanic lithosphere, continental lithosphere is buoyant with respect to the asthenosphere, resists recycling, is as old as 4 Ga, and is the archive of Earth history [19]. The bulk composition of the continental crust is similar to calc-alkaline andesite [20,21]. On the modern Earth, andesite is the characteristic rock type formed in the upper plate of convergent plate margins and constitutes the inferred major site for its formation in the past. Plate boundaries form a global, kinematically linked and dynamic system (figure 1) in which the total area of lithosphere generated at plate boundaries over medium- to long-term timescales is compensated by recycling back into the mantle, maintaining a constant-radius Earth.

The geological and geophysical manifestations of plate tectonics on the modern Earth are relatively well-studied and understood (for example, mid-ocean ridges and transform faults, rift zones, passive margins, Benioff zones, magmatic arc— trench systems, back arc basins, foreland basins, mountain ranges). However, extrapolating these established proxies of plate tectonics to the geological past is hindered by the lack of information from the oceans, increasing gaps in the geological record with increasing age, the lack of large-scale geometric constraints, and potential changes in the nature of the geological environment on the hotter early Earth, leading to uncertainty in the contribution of plate tectonics and/or non-plate tectonic processes to the long-term geological record (e.g. [5,9] and references therein). Plate tectonics is an ongoing, self-sustaining system of moving, interacting plates, and it is not always clear how to establish such a long-lived sustainable process from that preserved in the rock record.

3. Evidence for rigid lithosphere

Rigid lithosphere is taken to be a necessary pre-condition for plate tectonics. Higher mantle temperatures on the early Earth lead to models of lithosphere that is impregnated with magma and has reduced viscosity and rigidity, relative to the present day. Hence it is a poor medium for stress transmission [22–24]. Geologic evidence for the existence of significant areas of rigid lithosphere on the early Earth is provided by the stabilization of cratons, the accumulation of large sedimentary basins on subsiding stable substrates, and evidence for brittle fracturing and emplacement into the cratons by rectilinear dyke swarms [25–28]. These geological features

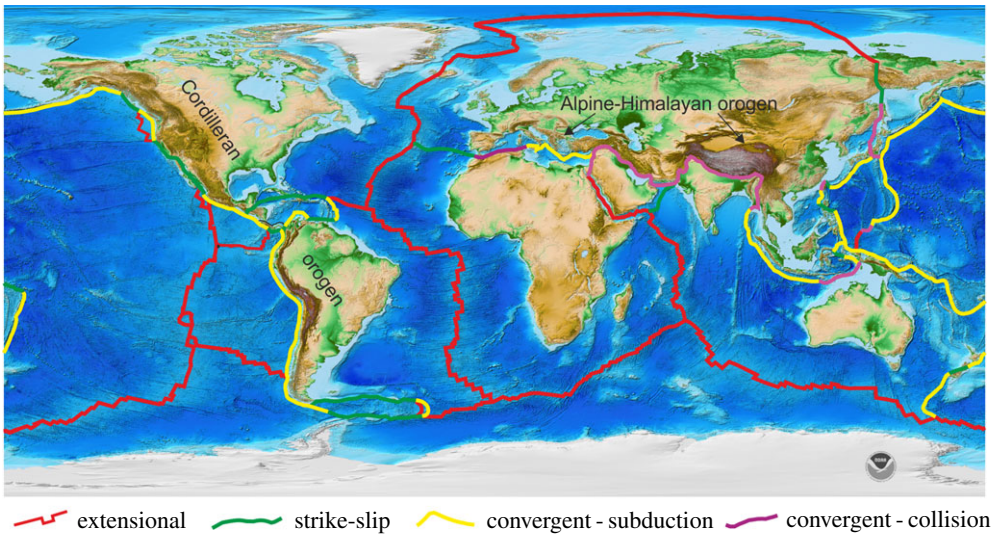

Figure 1. Present-day Earth global relief showing distribution of spreading, subduction, collisional and strike-slip boundaries. Global relief model based on National Oceanic and Atmospheric Administration (NOAA) ETOPO1 1 Arc-Minute Global Relief Model [11].

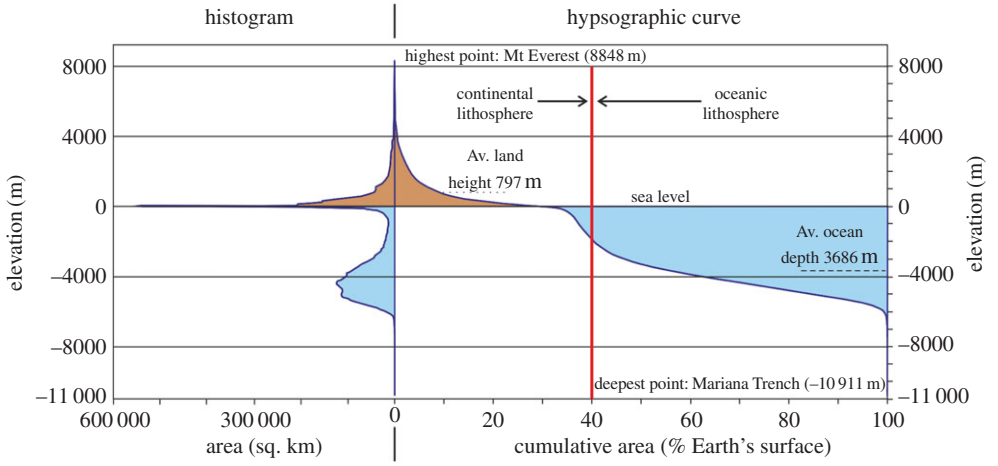

Figure 2. Histogram and hypsographic curve of land and ocean areas derived from ETOPO1 global relief model of Amante & Eakins [11].

extend back to the Mesoarchean, become more prevalent in the Neoarchean and are widespread in the Proterozoic (figure 3).

Extensive sedimentary basin successions overlying stable cratons include the *ca* 2640–2055 Ma Transvaal Supergroup on the Kaapvaal craton [29,30] and the 2775–2210 Ma Mount Bruce Supergroup on the Pilbara craton [31,32]. Older and geographically smaller basin accumulations on the Kaapvaal craton extend back to *ca* 3.2–3.0 Ga [33–38] and from *ca* 3.2 to 3.0 Ga for fluvial quartz arenites on the Dharwar craton [39]. Younger, predominantly Proterozoic examples include the *ca* 2610–2120 Ma Minas Supergroup, San Francisco craton [40], 2480–2220 Ma Huronian Supergroup on the southern Superior craton [41], *ca* 2450–1900 Ga Karelian Supergroup, Baltic craton [42] and late Palaeoproterozoic to Mesoproterozoic basins of India [43].

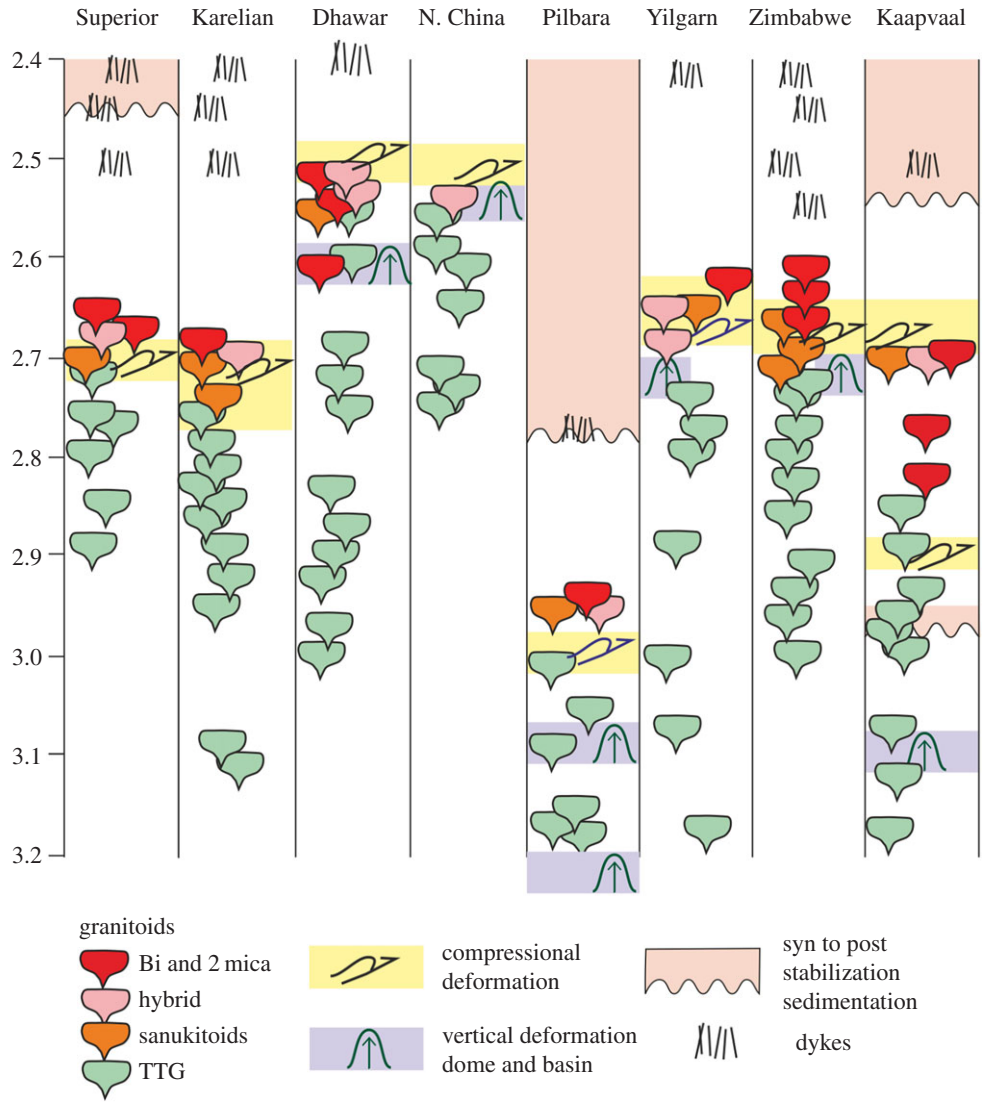

Figure 3. Time-space plot for the Superior, Karelian, Dhawar, North China, Pilbara, Yilgarn, Zimbabwe and Kaapvaal cratons for the period 3.2–2.4 Ga, showing the time of major pluton, mafic dyke emplacement and deformational events.

Fracturing and dyke emplacement events within cratons extend back to 3.5 Ga for the North Atlantic craton in Greenland [44] but only become widespread both within a craton as well as globally after *ca* 3.0 Ga. The Ameralik dykes of West Greenland and the equivalent Saglek dykes in Labrador are the oldest extensive mafic intrusions cutting stable continental crust [45]. U-Pb zircon dating of the Ameralik dykes indicate they do not represent a single event but yield ages of 3.5 Ga and 3.25 Ga [44]. Younger, post-craton stabilization events include the *ca* 3.0 Ga volcanic rocks at the base of the Pongola supergroup, Kaapvaal craton [46], the 2770 Ma Black range dykes and Mount Roe Basalt, Pilbara craton [31,47,48], the 2575 Ma Great dyke, Zimbabwe craton [49,50], the *ca* 2510 Ma and 2475 Ma dykes in the Zimbabwe, Superior and Kola-Karelia cratons [50], the 2420–2410 Ma dykes in the Yilgarn, Zimbabwe, Superior and Kola-Karelia cratons [50–52] and the 2370 Ma dykes, Dharwar craton [53] (figure 3). It is very striking that dyke swarms older than these are rare, which highlights the different nature of the continental lithosphere before 3 Ga. The synchronicity of late Archean and early

Palaeoproterozoic (*ca* 2.5–2.4 Ga) dyke emplacement events in the Zimbabwe, Kola-Karelia, Yilgarn and Superior cratons further suggests their spatial proximity within the inferred Superia supercontinent/supercraton [50,54].

Integrated geologic and seismologic studies of Archaean cratons indicate that they obtained their crustal and lithospheric thicknesses by the late Archaean with some intra- and intercratonic variability in thicknesses related to subsequent collision between blocks [12,55–58]. Furthermore, the secular evolution of granitoid composition from tonalite, trondhjemite and granodiorite (TTG) to K-rich metaluminous and peraluminous granites during the late Archean (3.0–2.5 Ga) as recorded in most cratons (figure 3, [59–61]) is further evidence for crustal thickening and reworking, and requires a rigid continental lithosphere by this time.

4. Geological evidence for plate margin interaction

Proxy data for interaction between moving lithospheric plates, whether divergent or convergent, are preserved in orogenic belts and results in distinctive patterns of geological features, which have variable long-term preservation potential. Interpretations of the Precambrian rock record must be modulated not only by an understanding of potential preservation bias, as in the skewing of sedimentary deposits towards epeiric intracontinental rather than craton margin deposits [62,63], but also by differences in parameters for the generation of rock associations. For example, the lack of vegetation resulted in braided channel environments across a range of basin depositional systems (fluvial, deltaic, tidal), carbonate accumulation mediated by changing biological controls (evolution), and the impact of secular cooling on the degree of mantle partial melting and crustal thermal regimes [62,64,65]. Even within such constraints, patterns of sedimentary, igneous, and metamorphic rock associations, and structural and metamorphic features associated with plate tectonic settings on the Phanerozoic Earth, are recognizable on the early Earth suggesting formation by similar tectonic controls.

(a) Divergent plate boundary record

The oceanic lithosphere record of plate divergence only extends back some 200 Ma, corresponding to a little over 4% of Earth's 4.56 Ga history. However, the record for continental lithospheric extension leading to break-up and sea-floor spreading extends back to the Archaean. Continental margin successions formed though lithospheric extension are divisible into rift (divergent plate) and thermal subsidence (intraplate) related basinal deposits (e.g. [66]). Rift-related facies associations consist of clastic, often terrestrial to lacustrine sedimentary units, including evaporites, with interstratified mafic and bimodal igneous rocks, and display rapid along and across strike changes in facies [67–70]. They unconformably overlie a now stabilized, pre-deformed and metamorphosed continental crust assemblage. Passive margin rock associations are composed of siliciclastic or platformal carbonates, in part reflecting palaeolatitude, with lateral continuity of facies types and constant stratigraphic thickness reflecting broad scale thermal subsidence of the rifted continental margin. The transition between rift and passive margin phases corresponds with the onset of sea-floor spreading and is marked by the break-up unconformity (figure 4*a*). Thus, the development of the earliest passive margin successions in the geological record provides a minimum age for bimodality of lithosphere into rigid continental and oceanic domains.

The oldest ages for the rift to drift transition are preserved in the North China, Zimbabwe, Pilbara and Kaapvaal cratons and give ages in the range *ca* 2750–2500 Ma [71–76]. For example, the *ca* 2.7 Ga Fortescue Group of volcanic and sedimentary rocks can be traced for some 500 km in an east-west direction along the southern margin of the Pilbara craton, unconformably overlying basement, and inferred to record crustal extension and subsequent break-up of the craton [71,77,78]. Furthermore, the long-term temporal distribution of ancient passive margin successions is episodic and are abundant at 2100–1850 Ma and 650–500 Ma, corresponding to the assembly phases of the Nuna and Gondwana supercontinents, but are scarce during Rodinia

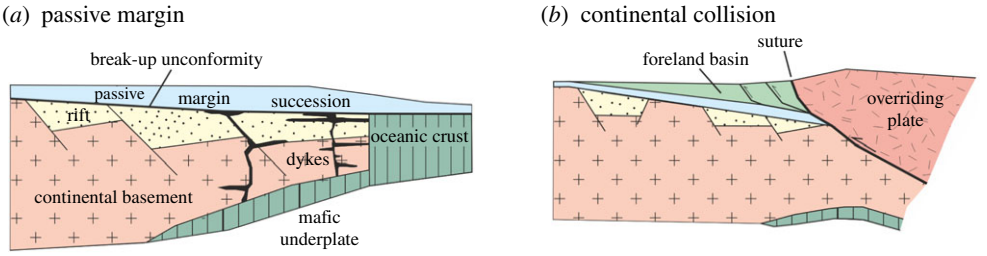

Figure 4. Schematic cross sections of (*a*) passive continental margin showing transition from rift to thermal subsidence phases marked by break-up unconformity and the onset of sea-floor spreading, and (*b*) continental collision resulting in loading and subsidence of lower plate and development of foreland basin succession.

assembly and are absent prior to 3 Ga (figure 5*a*; [67]). The purported oldest passive margin succession is in the Steep Rock carbonate platform, which unconformably overlies the tonalite basement of the Superior craton, but sediment accumulation is only poorly constrained between 3.0 and 2.8 Ga [67,85]. The temporal distribution of passive margins is in part mimicked by that of carbonates, which are generally associated with extensional tectonic settings, and are largely younger than 2800 Ma [86]. We consider the episodic temporal distribution pattern of passive margins to reflect selective preservation during the supercontinent cycle [19,87,88].

(b) Convergent plate boundary record

Divergent lithospheric motion must be compensated by lithospheric recycling at convergence margins on a constant-radius earth. Convergent plate boundaries include subduction zones in which oceanic lithosphere is recycled back into the mantle beneath an upper plate of either oceanic (e.g. West Pacific) or continental (e.g. Andes or Japan) lithosphere, and collision zones in which opposing plates of buoyant continental lithosphere resist and ultimately terminate subduction (e.g. Alpine-Himalayan belt, figure 1). These contrasting convergent boundary types are preserved in accretionary and collisional orogens; the former generated at sites of ongoing subduction and the latter at the termination of subduction [89,90]. Each orogen type is characterized by distinctive lithotectonic assemblages, which are aligned in long linear belts parallel to the inferred plate boundary (figure 1).

(c) Foreland basins

Foreland basins form in convergent plate settings due to lithospheric loading driven subsidence (figure 4*b*; [66,91,92]). Basin fill includes detritus from the thickened crustal pile of the overriding plate. The oldest inferred examples occur at around 3.0 Ga and include the Witwatersrand Basin, South Africa, the Cheshire Formation of the Belingwe Greenstone Belt, Zimbabwe and the Pontiac Basin, Canada. They are characterized by siliciclastic-dominated sedimentary succession, with lateral facies and thickness variations reflecting syn-sedimentary tectonic instability including disruption of the basin succession by thrust faults and/or tectonothermal events in adjoining blocks with the developing orogenic belt then acting as a sediment source. The late Mesoarchaean (3.0–2.8 Ga) Witwatersrand Basin formed during amalgamation and stabilization of the Kaapvaal craton in southern Africa, and it contains detritus derived from the bounding exhumed cratonic blocks and accreted granite-greenstone terranes (e.g. Barberton and Kimberley [26,34,38]). Facies and stratigraphic relations for the 2.65 Ga Cheshire Formation of the Belingwe Greenstone Belt are interpreted to indicate a lower carbonate succession, representing passive margin sedimentation on an older continental rift succession, and an upper siliciclastic succession that accumulated in an asymmetric basin [73]. The basin was deformed soon after sediment accumulation by north-directed thrusts and is interpreted as a foreland basin formed ahead of a northwest advancing

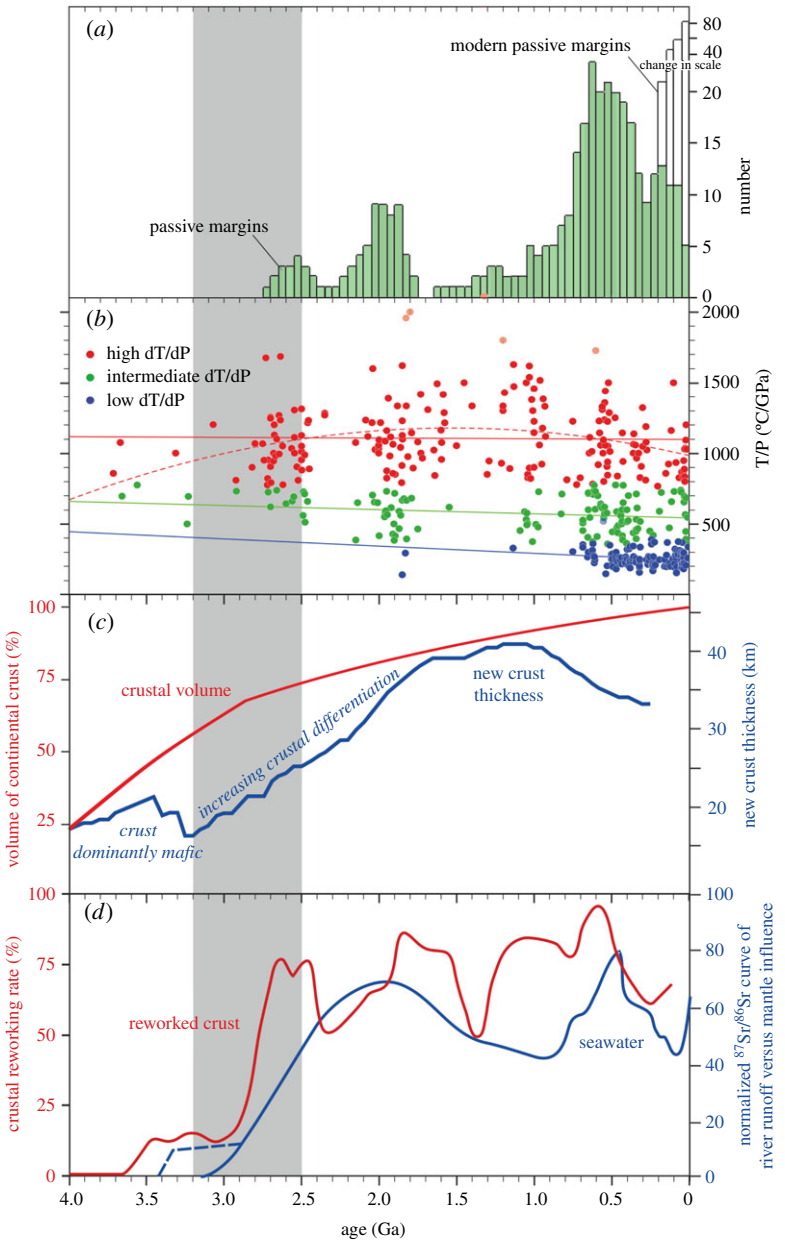

Figure 5. (*a*) Histogram of the ages of ancient and modern passive margins [67]. (*b*) Metamorphic thermal gradient (*T*/*P*) for 456 localities grouped as high d*T*/d*P* in red, intermediate d*T*/d*P* in green and low d*T*/d*P* in blue, and plotted against age [64]. (*c*) Crustal growth model based on Hf isotope ratios in zircons [79] and a shift in the composition of juvenile crust from mafic to more intermediate compositions accompanied by an inferred increase in crustal thickness [80]. (*d*) Moving average of δ18O analyses of zircon versus U-Pb ages distilled from compilation of approximately 3300 [81] and normalized seawater $^{87}Sr/^{86}Sr$ curve [82], incorporating data of Satkoski *et al*. [83,84]. Grey bar highlights age range 3.2–2.5 Ga.

thrust stack [93]. Foreland basins settings have also been proposed for Neoarchaean sedimentary successions (*ca* 2.7 Ga) in the Superior Province of Canada, and are unconformably overlain by molasse basin deposits marking stabilization of the craton [94,95]. Proterozoic foreland basins have been described from Africa, Australia, India and Canada [26,63,96].

(d) Metamorphic assemblages

Metamorphic mineral assemblages provide a record of heat flow within the crust at the time of their formation, which in turn is a function of tectonic environment. A compilation by Brown & Johnson [64] of temperature, pressure, thermal gradients and age of metamorphism for mineral assemblage from some 450 localities ranging in age from Eoarchaean (less than 3800 Ma) to Cenozoic (less than 65 Ma) is divisible into three groups based on their thermal gradients (figure 5*b*): high dT/dP with thermal gradients of greater than 775°C GPa^{-1} resulting in upper amphibolite and granulite facies, and ultrahigh temperature (UHT) metamorphic rocks; intermediate dT/dP with thermal gradients of 375–775°C GPa^{-1} and producing eclogite, high pressure granulite and high pressure amphibolite facies rocks; and low dT/dP with thermal gradients of less than 375°C GPa^{-1} associated with blueschists, low temperature eclogites, and coesite and diamond facies ultrahigh-pressure (UHP) metamorphic rocks. The latter assemblages are largely restricted to Cryogenian (less than 850 Ma) and younger aged rocks [97], except for three Palaeoproterozoic (*ca* 1.8 Ga) examples [98–100] and one Mesoproterozoic (*ca* 1.14 Ga) example [101]. Brown & Johnson ([64] and references therein) argue that the intermediate and high dT/dP gradients represent temporally paired systems that commenced at the end of the Mesoarchaean (less than 2800 Ma). The intermediate thermal gradients are attributed to subduction and collisional settings, and the higher gradients with the hinterland of the overriding plate (e.g. high T back arc environments; cf. [102]) or oceanic plateaus.

Stevens & Moyen [103] describe a spatially linked paired metamorphic belt (*ca* 3.2 Ga) from the Palaeoarchaean Barberton granite-greenstone terrane. In the recent geologic past, paired metamorphic belts are related spatially as well as temporally, and the implications of paired systems only known to be linked temporally are still being debated. Low dT/dP assemblages, represented by rock types such as blueschists, are linked to the subduction of cold oceanic lithosphere, which depress geotherms, and are taken as indicative of contemporary convergent plate interaction associated with secular cooling of the mantle [3]. UHP coesite and diamond-bearing assemblages are modelled within a cooler mantle environment (less than 100°C higher than present-day mantle potential temperatures), which enables a deeper level of detachment of the oceanic plate lithosphere from the lower continental lithosphere during continent-continent collision [104].

(e) Deformation features

The boundaries of lithospheric plates on the present-day Earth are long curvilinear features (figure 1) with stress transmitted through the rigid plates and focused at boundaries as evidenced by the distribution of earthquake foci. Coupling across convergent boundaries results in crustal thickening and stabilization forming accretionary and collisional orogens (e.g. Cordillera and Alpine-Himalayan belts, figure 1). Within these mountain belts sedimentary, deformational, metamorphic and magmatic elements are aligned parallel to the orogen reflecting the temporal and spatial integration of processes associated with initial tectonic setting (e.g. continental rifting, passive margin formation, subduction initiation) and those associated with the stabilization of these pre-existing tectonic associations into the geological archive (e.g. crustal thickening and metamorphism of plate margin assemblages during orogenesis) [89,105,106]. Long, linear accretionary and collisional orogens are recognized throughout the Phanerozoic and Proterozoic and are testimony to the operation of long, linear plate boundaries reflecting horizontal motions of plates through Wilson cycles of oceans opening and closing; for example, the largely Phanerozoic Variscan, Appalachian-Caledonian, Uralian, Terra Australis and Central Asian orogens, and the Proterozoic Cadomian, East African-Mozambique, Grenville-Sveconorwegian-Sunsas, Mazatzal-Yavapai, Svecofennian, Capricorn, Trans-Hudson, Trans-North China, Eburnean, Karelia, Akitan and Aldan orogens.

In contrast with modern orogenic belts, those preserved in Archaean cratons are small with limited along strike extent, and as a consequence the orogenic tracts lack pronounced length

to width ratios. However, the original extent of the cratons has been modified by subsequent cycles of continental accretion and dispersal. For example, the Yilgarn craton consists of a series of largely linear granite-greenstone belts that were assembled through late Archaean accretionary events [107,108]. The belts have an overall north-south trend but are truncated along the northern and southern margins of the craton resulting in a present-day equidimensional aspect ratio but indicating a greater and unknown original linear extent. Thrust faults and associated asymmetric folding are features of a number of Archaean blocks (e.g. southwest Greenland, southern Africa, Yilgarn) and consistent with models involving extensive horizontal shortening [109–111] forming linear structural patterns that can be traced for hundreds if not thousands of kilometres across at least late Archaean cratons [112,113]. The Greenland example consists of a thrust stack of Meso- and Neoarchaean high-grade gneisses separated by mylonites which indicate top to the northwest sense of movement that is constrained to around 2.7 Ga on the basis of synkinematic granite sheets intruded along the mylonites [110]. Furthermore, Komiya *et al*. [114] argue on the basis of mapping in the northern part of the Isua Belt, West Greenland, for an inferred ocean floor stratigraphy of basalt, chert and turbidites repeated across strike by low-angle thrusts. They interpret this lithotectonic association to represent an accretionary complex formed at a plate boundary trench through off-scrapping of the upper crustal portion of subducted rigid oceanic lithosphere. Inferred ocean floor and trench deposits have also been mapped within the 1300 km-long accretionary orogen in the central segment of the North China Craton [115,116].

At a crustal scale, seismic reflection profiles have been used to invoke horizontal Archaean crustal shortening; for example, a profile from the southern Superior craton across the boundary between the Opatica Plutonic Belt and the Abitibi Greenstone Belt. North-dipping reflectors can be traced from near the base of the Abitibi Belt northward to 65 km below the Opatica Belt and they are interpreted to represent either a fossil subduction zone [117,118] or delaminated lower crust that formed in response to a collisional event further south [119].

Although some cratons consist of accreted linear granite-greenstone terranes, others are characterized by dome and keel structures resulting in an original equidimensional outcrop pattern. For example, the eastern Pilbara, Zimbabwe and Dharwar cratons consist of semi-circular granitoid domes flanked by low-grade synclinal belts of volcanic and volcaniclastic greenstones that dip and face away from the cores of the domes, with an overall radial mineral stretching lineation [120–123]. These features are interpreted to form through vertical, diapiric motion of granitoid bodies (figure 3) driven by density contrasts between granitic crust beneath a thick, dense and insulating greenstone cover succession [124,125]. Dome and keel structures contrast with fold and thrust belts related to horizontal motion of the lithosphere and which characterize crustal development in younger orogens. In the well-studied East Pilbara region, pluton emplacement and doming extended over hundreds of millions of years, not just across the craton as a whole but also within individual plutons [126,127]. Dome and keel structures in the Pilbara ceased around 3.1 Ga and were replaced by linear structural patterns related to horizontal tectonics [128]. The timing of this change also corresponds with a change in geochemistry from within-plate-like igneous rocks to rocks with subduction-related signatures [129]. In the Dharwar craton, India, dome and basin structures are related to lateral constructional flow in the lower crust of a hot orogen [130]. These structures formed at around 2.6 Ga [131–134], although the stratigraphic and provenance record of sedimentary units within the craton suggest a stable craton as early as 3.0 Ga [135]. Diapiric emplacement of *ca* 2.75 Ga granite gneiss into greenstone cover occurs locally in the western part of the Yilgarn craton [136]. Dome and basin structures are associated with *ca* 2.5 Ga granite-greenstone terranes in the Eastern Block of the North China craton [116,137,138], with structural analysis suggesting vertical motion of granite domes between synclinal greenstone belts [139,140].

(f) Magmatic record of subduction

Igneous rocks have geochemical signatures related to their source composition and the nature of the melting process, and these in turn reflect the tectonic setting in which they were generated

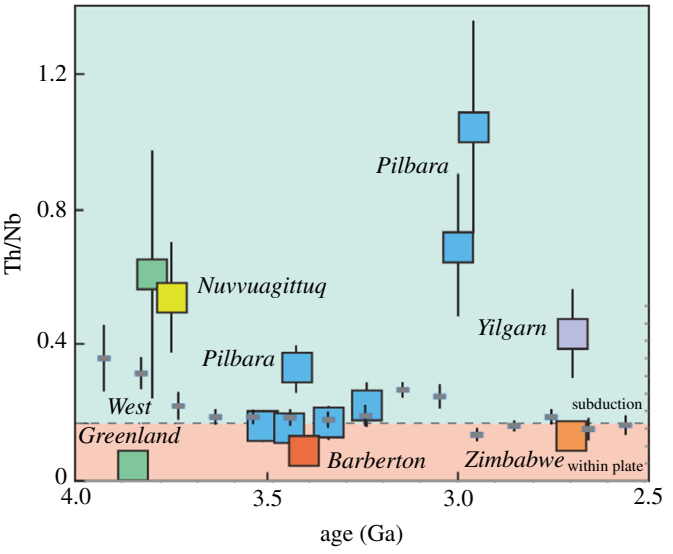

Figure 6. Mean Th/Nb ratios of suites of Archaean predominantly mafic rocks which are thought not to have been modified significantly by crustal contamination, after Dhuime *et al.* [153]. The green field is for elevated Th/Nb ratios, which are attributed to subduction-related processes, and the orange field is for within plate magmas. We note that in terms of mass balance it is easier to develop high Th/Nb ratios by the introduction of some from of contaminant (e.g. of pre-existing crust), than it is to develop low Th/Nb ratios by a contamination process. Data from: Barley *et al.* [154], Smithies *et al.* [150,155], O'Neil *et al.* [156], Jenner *et al.* [157,158], Puchtel *et al.* [159], Shimizu *et al.* [160] and de Joux *et al.* [161]. The small squares with different colours reflect the different locations plotted. Also plotted are the mean Th/Nb data in 100 Ma time slices (grey boxes) from a global dataset from Keller & Schoene [65].

[141,142]. This is particularly well established for more mafic rock types, with subduction-related igneous rocks characterized by negative anomalies in Nb and Ta in mantle normalized minor and trace element patterns, and hence elevated Th/Nb and Th/Ta ratios [141]. Such geochemical discriminants work well in characterizing subduction zone rocks over the recent geologic past but their applicability to the early hotter Earth is less certain. This has led to both plate tectonic and non-plate tectonic models for early continental crust generation [143–147]. Moyen & Laurent [148] noted that Archaean mafic rocks are often clustered between subduction and non-subduction compositions, relative to those on the modern Earth, suggesting that true subduction systems may have been rare.

Nonetheless, trace element ratios that are not strongly affected by variable degrees of mantle melting have been used to evaluate tectonic settings in the Archaean. Nb and Th have similar incompatibility during mantle melting and Th/Nb ratios greater than 0.2 are associated with subduction-related processes associated with the release of fluids or melts from the subducted slab [65,141]. Using a weighted bootstrapped resampling methodology of a global dataset, Keller & Schoene [65] noted little change in average Th/Nb ratios through time, and concluded that subduction-related magmatism had been ongoing throughout much of Earth's history. Other studies have recognized the presence in Archaean successions of boninitic magmas [144,149–151], and in some cases lithostratigraphic associations [152], similar to those found in more recent subduction-related settings. However, the results of detailed case studies (figure 6, and references) suggest that magmas associated with subduction and with intraplate tectonic settings were generated in different areas in the period 3.8–2.7 Ga, and also that there may be a link between dome and keel tectonics and intraplate magmatism, at least in some of these areas.

Figure 6 illustrates the tectonic settings inferred from a number of different case studies in different locations in the Archaean, and compares them with the global compilation of Th/Nb ratios from Keller & Schoene [65]. The studies depicted have used both major element and trace

element proxies, and the point is not to interrogate those approaches further but to look at their outcomes and potential implications for geodynamics. Subduction-like magmatism has been recognized in West Greenland and the eastern Superior Province at approximately 3.8 Ga, and then later in the Pilbara of NW Australia at less than 3.1 Ga [129,152,157,162,163]. Magmatism with no significant subduction signal, here termed intraplate even though it may have been too early for plates to have been established, has in turn been documented in West Greenland, and in younger rocks in Barberton, Pilbara and Zimbabwe [129,158–160,164]. Moreover, in the last three examples, the intraplate geochemical signature is associated with dome and keel exposures indicating vertical tectonics. In a number of areas, subduction-like geochemical signatures extend into, and become more widespread, in younger Archaean sequences, most notably the Superior Province ([165]; but see Bédard *et al*. [166], for an alternative view [167]), the Pilbara [129], parts of the Yilgarn [168] and the North China Craton [169]. Similarly, Archaean plutonic rocks are the sodic-rich TTG suite, and are not replaced by more potassic and peraluminious plutonic rocks, typical of modern tectonic environments, until the latter part of the Archaean (figure 3; [59]).

5. Palaeomagnetism and lateral motion of Archaean continental blocks

Cawood *et al*. [2] and Evans & Pisarevsky [27] analysed available Archaean and Palaeoproterozoic palaeomagnetic data to test the existence of plate tectonics at those times. Both sets of analyses have been positive, but with some reservations concerning the quality and reliability of those data. For example, 2687 ± 6 Ma Mbabane Pluton pole [170] is not supported by field test and it is also located suspiciously close to younger poles. The Kaapvaal Ongeluk Lavas pole [171] has been recently re-dated [172]. On the basis of such revisions, along with new palaeomagnetic data, we have chosen a series of poles for testing the possibility of mutual lateral motions of cratonic blocks in the late Archaean to early Palaeoproterozoic. These are datasets on the oldest rocks currently available. We found three time intervals around 2680 Ma, 2505 Ma and 2440 Ma that contain coeval reliable palaeomagnetic data from the Superior and Kola-Karelian cratons with additional reliable palaeopoles also reported from the Kaapvaal craton for *ca* 2680 and 2440 Ma (table 1). There are also two coeval pairs of 2780 Ma and 2720 Ma palaeopoles from Kaapvaal and Pilbara (table 1).

Following the method used by Cawood *et al*. [2] and Evans & Pisarevsky [27], we made a series of palaeomagnetic reconstructions of: (i) Superior and Kola-Karelia at 2680 Ma, 2505 Ma and 2440 Ma (figure 7*a–c*); (ii) Superior and Kaapvaal at 2680 Ma and 2440 Ma (figure 7*d*,*e*); and (iii) Kola-Karelia and Kaapvaal at 2680 Ma and 2440 Ma (figure 7*f*,*g*). In all reconstructions, we fixed one of the two tested cratons and show schematically two polarity options (solid and dashed lines) together with longitudinal uncertainty (three possible positions along the same latitude) for the other craton. These reconstructions reveal that mutual movements of the tested cratons occurred sometime between 2680 Ma and 2440 Ma. Figure 7*h*,*i* demonstrates the same test for Pilbara and Kaapvaal for 2780 and 2720 Ma. As the palaeopoles for these two cratons suggest high latitude positions, we have shown only one polarity option. We also consider this test as positive, but admit that large circles of confidence theoretically permit reconstructions with the same mutual position of the two cratons at 2780 Ma and 2720 Ma, if we allow minimal overlap of the circles of confidence (expressed at the 95% level). Owing to longitudinal uncertainty and polarity ambiguity it is not easy to estimate the relative scale of movements of the tested cratons. However, using the reconstructions of Superior and Kaapvaal at 2680 Ma and 2440 Ma, which have the most precise palaeopoles with small circles of confidence, we estimated minimal distance of their mutual movement between 2680 and 2440 Ma. We chose the closest possible position of the two cratons at those ages and show them in Superior coordinates (figure 8). The shortest possible movement of Kaapvaal with respect to Superior is along a small circle (the pole of this circle is shown in red and the reference point in black) with the radius of about 16° by about 170° clockwise. This will require about 5100 km of movement of the reference point. All other options for these two cratons between these two time periods suggest larger distances. We conclude that

Table 1. Palaeomagnetic data. Hiage and Lowage indicate the age range of the studied rocks. Tests refer to palaeomagnetic field tests indicating the primary remanence [173] for assessing the reliability of palaeomagnetic data. Plat, Plong and A95 refer to the measured latitude and longitude of palaeomagnetic poles and their 95% confidence circle.

Craton and age bracket	rock name	Hiage	Lowage	tests	Plat	Plong	A95	reference
2780 Ma								
Kaapvaal	Derdepoort Basalt	2787	2777	G+	−39.6	004.7	17.5	Wingate [174]
Pilbara	Black Range Dolerite Suite	2774	2770	G*+,C*+	−3.8	130.4	15.0	Evans *et al*. [175]
2720 Ma								
Kaapvaal	Westonaria Basalts	2722	2706		−17.1	047.9	18.5	Strik *et al*. [176]
Pilbara	Pilbara Flood Basalts, Packages 8–10	2721	2710		−59.1	186.3	6.1	Strik *et al*. [177]
2680 Ma								
Superior	Otto Stock Dykes and Aureole	2679	2681	C*+,R−	69.0	227.0	4.8	Pullaiah & Irving [178]
Kola-Karelia	Koitere Sanukitoids	2686	2682		−68	192.5	19.5	Mertanen & Korhonen [179]
Kaapvaal	Rykoppies Dykes	2685	2681	C+	−62.1	336.0	3.8	Lubnina *et al*. [180]
2505 Ma								
Superior	Ptamigan Mean	2507	2503		−45.3	213.0	13.8	Evans & Halls [181]
Kola-Karelia	Shalskiy Gabbronorite Dyke	2512	2504	C*+	22.7	222.1	11.5	Mertanen *et al*. [182]
2440 Ma								
Superior	Matachewan N	2449	2443	C+	52.3	239.5	2.4	Evans & Halls [181]
Kola-Karelia	Avdeev Gabbronorite, Shalskiy Dyke	2510	2441	C*+	−12.3	243.5	14.0	Mertanen *et al*. [182]
Kaapvaal	Ongeluk lava and related intrusions	2429	2423	G*+	04.1	282.9	5.3	Evans *et al*. [171]; Gumsley *et al*. [172]

there is compelling evidence for significant relative horizontal movement between cratonic blocks by the late Archaean.

6. Late Archaean changes in character of continental lithosphere

Sedimentological, structural, magmatic, metamorphic and palaeomagnetic datasets provide proxy evidence for lateral motion of continental lithosphere extending back until at least 3 Ga, with selected geochemical discriminant data, such as Th/Nb, inferred to represent supra-subduction zone settings at least locally as old as 3.8 Ga. Furthermore, regional and global datasets for the continental crust and its lithospheric mantle indicate significant changes in its character during the Meso- to Neoarchaean (3.2–2.5 Ga; for example, figures 3 and 5).

(a) Continental crust composition and thickness

The continental crust has evolved from a dominantly mafic composition prior to 3.0 Ga to an andesitic composition today. For example, Tang *et al*. [183] used Ni/Co and Cr/Zn ratios in

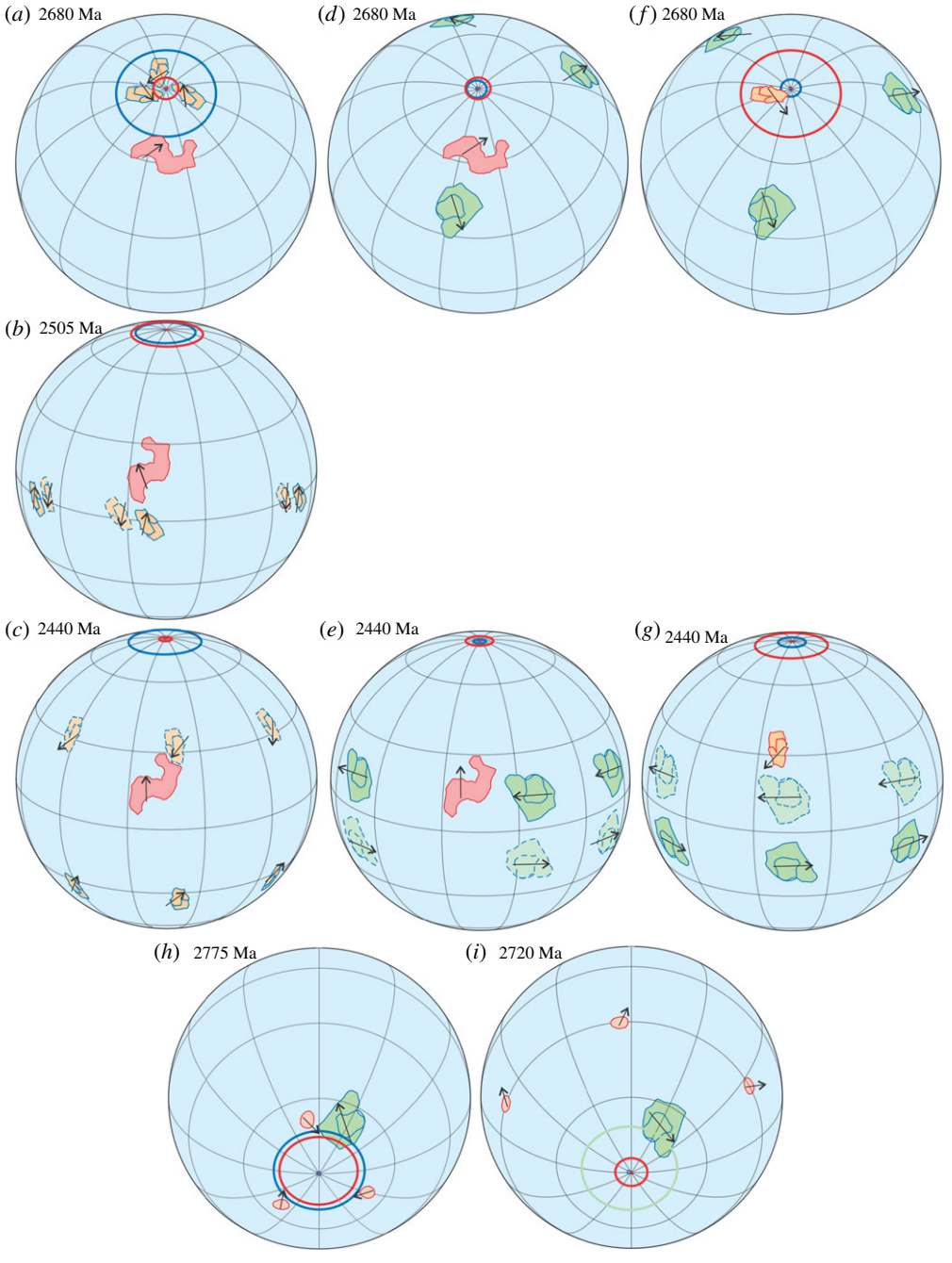

Figure 7. Palaeomagnetic reconstructions of Superior, Kola-Karelia and Kaapvaal cratons at 2680 Ma (*a*,*d*,*f*), 2505 Ma (*b*), 2440 Ma (*c*,*e*,*g*); of Kaapvaal and Pilbara cratons at 2775 and 2720 Ma (*h*,*i*). Arrows denote directions to the present data north. Alternative polarity option is shown with dashed outlines. See also text.

Archaean sedimentary and igneous rocks as a proxy for bulk MgO composition of the Archaean upper continental crust. It remains difficult to tie down the extent to which the rocks sampled by greenstone belt sediments are representative of the upper crust. Nonetheless, Tang *et al*. [183] concluded that this crust had an initial MgO content of *ca* 15% prior to 3 Ga, corresponding to a mafic bulk composition, but had a MgO content of *ca* 4% by 2.5 Ga, similar to modern felsic upper

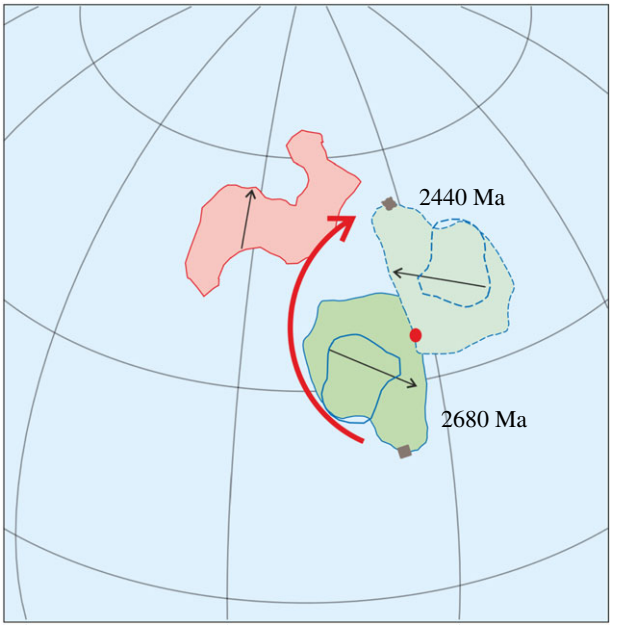

Figure 8. Palaeomagnetic reconstructions of Superior and Kaapvaal cratons at 2680 and 2440 Ma (in the Superior coordinates) with minimal distance between the two cratons.

continental crust. Compiled records of Cr/U in terrigenous sediments suggest derivation from predominantly mafic crust prior to 3 Ga followed by a 0.5–0.7 Ga transition to crust of modern andesitic composition [184]. Similarly, statistical modelling from a database of 70 000 analyses of igneous rocks preserved within the continental crust reveal a significant change in secular trends at around 2.5 Ga inferred to involve a decrease in mantle melt fraction in basalts, and in indicators of deep crustal melting and/or fractionation (Na/K, Eu/Eu* and La/Yb ratios in felsic rocks, [185]).

The rapid shift in elemental abundances relative to the progressive decrease in mantle temperature around the Archaean–Proterozoic boundary indicates mantle temperature alone cannot be the driver for these changes [65], and are consistent with changes in processes of crust generation. Dhuime *et al*. [80] documented a progressive increase in the median Rb/Sr content of igneous rocks at the time of their extraction from the mantle, from relatively low values prior to 3 Ga rising to maximum values between 1.8 to 1.0 Ga. There is a positive correlation between Rb/Sr ratio, SiO_2 content, and thickness of crust for the compiled dataset [80]. The changing Rb/Sr equates to SiO_2 content and thickness of new continental crust, increasing from *ca* 48% and 20 km before 3.0 Ga to more intermediate compositions of up to *ca* 57% and 40 km thick crust by 1.8 Ga before decreasing after 1 Ga to values of 55% and 30 km towards the present (figure 5*c*). By contrast, Greber *et al*. [186], using δ^{49}Ti isotopic composition of shales, which they argue is a proxy for SiO_2 content of the source, noted values that are both similar to felsic rocks as well as relatively constant over the last 3.5 Ga. Thus, they proposed that felsic rocks have been a dominant component of the eroding crust throughout this timeframe, and that the source of these fractionated compositions was plate tectonics.

(b) Continental crustal reworking, recycling and subaerial exposure

Temporal variations in U-Pb, Hf and O isotopes in detrital zircons (for example, [79,81]) have been used to assess the relative contributions of new and reworked continental crust. Global compilations of δ^{18}O in zircons show a marked departure away from mantle values after

the Archaean [81,187], which is taken to indicate significant continental crustal reworking (and increasing crustal thickness) since that time. Spencer *et al*. [81] concluded that the highest proportion of reworked crust corresponded with periods of continent/supercontinent amalgamation and the proportion of reworked crust was uniformly low prior to about 2.7 Ga (figure 5*d*). Periods of supercontinent assembly are taken to reflect periods of continental convergence, assembly and thickening, resulting in reworking of continental lithosphere. The generally low $\delta^{18}O$, juvenile Hf isotopic values in the Archaean implies little in the way of crustal thickening associated with collision-related orogenesis and reworking.

Dhuime *et al*. [79] used zircon isotopic data to argue for a decrease in the rate of continental growth at around 3.0 Ga. Assuming that new continental crust has been generated at a broadly constant rate since say 4 Ga, the decrease in the rate of crustal growth at approximately 3 Ga is attributed to an increase in the rates at which continental crust is destroyed—along destructive plate margins (figure 5*c*; [153]). In a similar vein, inclusions in continental sub-lithospheric mantle diamonds display a major change at around 3 Ga with the incoming of eclogitic inclusions [188]. Eclogite provides evidence of the return of the basalt protolith to the mantle, which Shirey & Richardson [188] related to the onset of subduction but could equally be achieved via any mechanism for crustal foundering, such as delamination.

Isotopic proxies of seawater composition indicate a change towards the end of the Archaean that is related to the widespread emergence of continental crust. The $^{87}Sr/^{86}Sr$ ratio of carbonates deviates from contemporaneous mantle values by 3 Ga and possibly as early as 3.2 Ga (figure 5*d*) [83,189]. Similarly, $\delta^{66}Zn$ values and the Nd-Hf isotopic composition of banded iron formation deviate from mantle values and shifting towards values for modern seawater by around 2.7 Ga [190,191]. These observations require the emergence and erosion of a significant area of evolved crust suggesting that by around 3.2–2.7 Ga the rheology of the continental crust was sufficiently rigid to enable it to record dyke swarms, be thickened, and become emergent (cf., [192,193]). The temporal distribution of LIP is also indicative of significant crustal emergence around this timeframe [28]. If Archaean greenstone belts are LIPs, they are largely submarine [194]. The first subaerial LIPs occur around 3 Ga in the Pilbara and Kaapvaal cratons and they become widespread across all cratons by the end of the Archaean, consistent with a major period of continental thickening and stabilization [195].

(c) Linking geological proxies with geodynamic modelling

Late Archaean changes in the bulk composition and thickness of continental crust along with increasing amounts of reworking and recycling of the crust, its widespread subaerial exposure (figure 5), and the emplacement of dyke swarms, are indicative of stabilization of the cratons. Additional expressions of this stabilization include a change from sodic TTG magmatism to K-granites and peraluminious granites [59]. These changes in granitoid composition are often co-incident with pulses of regional deformation and metamorphism followed by a termination of tectonothermal activity and isolation of the craton from subsequent tectonic events (figure 3). The timing of these changes are not synchronous but vary from craton to craton; for example, *ca* 3.7 Ga in parts of the North Atlantic, 3.0 Ga in the Pilbara, 2.9 Ga in the Amazon, 2.85 Ga in the Kaapvaal, 2.75 in the Karelia, 2.7 Ga in Superior and Yilgarn, and 2.6 Ga in Dharwar, and 2.55 Ga in North China.

Late Archaean changes in composition and character of rock associations occur within a framework of decreasing mantle potential temperature [196,197], which is associated with a change in mantle viscosity and lithospheric rigidity [192]. Although absolute values for mantle potential temperature in the Archaean are debated (e.g. [197–199]), all involve secular cooling since at least 3 Ga, which would result in lower degrees of partial melting of the mantle and less melt impregnation within the lithosphere (cf. [23]). Secular cooling impacts on mantle viscosity, which along with increasing rigidity of the lithospheric lid [200,201], will lead to an increase in the wavelength of mantle convection, which in turn feeds back into the mechanism of heat transfer [202]. Plate tectonics is associated with mantle convection of wide aspect ratios [203], whereas

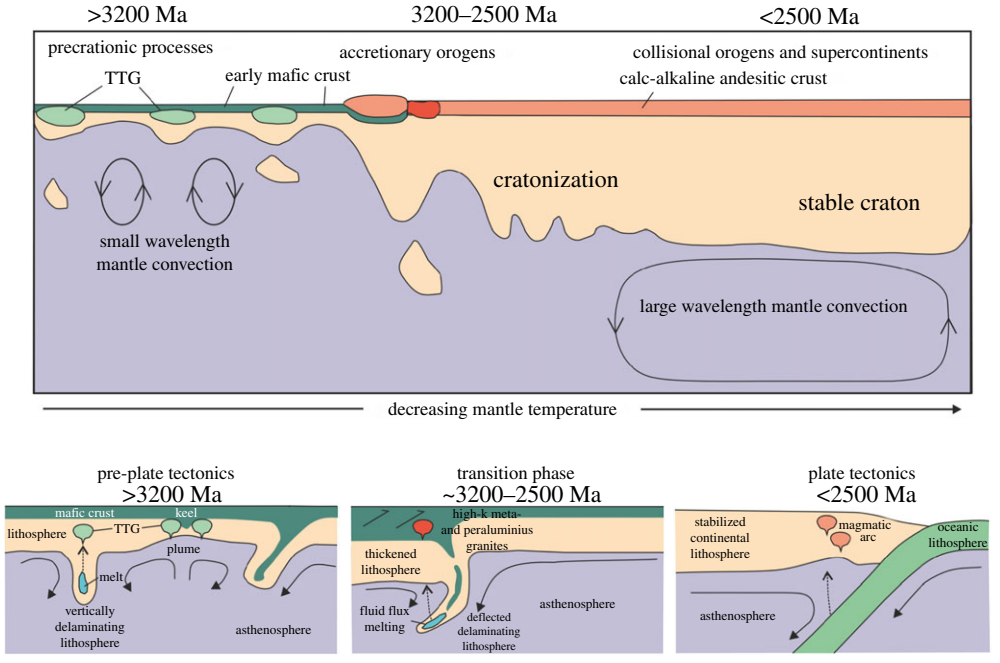

Figure 9. Schematic temporal evolution of the lithosphere associated with decreasing mantle temperature. Early Earth, prior to 3.2 Ga involves a non-plate tectonic regime, with magmatism characterized by a bimodal association of TTG (tonalites, trondhjemites and granodiorites) and greenstone belts. Mantle plumes are a major source of mafic magmatism. Recycling occurs through delamination and mantle convection is of relatively small wavelength. Subduction where present is transitory. Plate tectonics is envisaged to have commenced after 2.5 Ga and is associated with large aspect ratio mantle convection. Between these two tectonic regimes is a transition phase in which the lithosphere is stabilized, differentiates into oceanic and continental types, with the latter undergoing thickening enabling its emergence and erosion.

the hot early Earth, whether operating in a stagnant-lid or in some other mode, would have had more vigorous convection of shorter wavelength and aspect ratio beneath a relatively viscous lid impregnated by plume-related igneous activity [204–206].

Production of continental crust, largely dominated by production of sodic TTG plutons resulted in differentiation of the lithosphere from an early largely mafic mono-lithologic crust into oceanic and continental types with contrasting density and thickness profiles. Cooling, melt extraction and dehydration of the Archaean lithosphere resulted in stabilization [55,56] of increasing volumes of continental lithosphere [79,207], which combined with their thermal blanketing effects on the convecting mantle [208,209], enable effective stress transmission through the lithosphere and its focusing at cratons' margins [210], breaking the lithosphere into plates and the formation of subduction zones [211]. Thus, we speculate that the observed changes in the geological archive in the late Archaean, in association with secular mantle cooling, corresponds with a change from a poorly mobile to a mobile lithosphere, and the reorganization of short to long wavelength mantle circulation. This marks the transition to a regime with a global pattern of linked plate boundaries, enabling sustained plate motions, and commencement of the large-scale continental assembly and dispersal. This evolving geodynamic scenario is shown schematically in figure 9.

The staggered timing between cratons in the development of different types of sedimentary basins, structural styles, metamorphic patterns and igneous rock associations and their geochemical signatures (for example, figure 3) suggest that the change from a non-plate tectonic mode to plate tectonics transitioned over some 500 to 700 Myr between *ca* 3.2 Ga and 2.5 Ga (cf. [8]). Localized and episodic subduction may have taken place prior to this transition based on

geochemical signals [152,157], numerical modelling constrained from Archaean lithostratigraphic assemblages [212], modelling of major meteorite impacts [213,214], and compression around the margin of plumes [215]. Within the caveat of a fragmentary and incomplete geologic record, these inferred early pulses of subduction are not considered to form part of a globally linked system of divergent and convergent boundaries. The episodic nature of this early subduction likely reflects the infrequent nature of the driving mechanism (for example, meteorite impact), the hot nature of the mantle leading to slab breakoffs, which prevented the development of a sustained slab-pull driver for ongoing subduction, and the localized and time-limited nature of the compressive force (mantle plume) resulting in transient and non-self-sustaining subduction. In this pre-plate tectonics regime, crust formation and dehydration progressively increased the rigidity of sizeable blocks of lithosphere. Once entrained in the mantle convection pattern, the blocks could widen, migrate at larger rates, and undergo thickening and compression at their margins as they assembled, whereas other regions remained in the undeformed, poorly mobile lid tectonic mode.

7. Conclusion

Arguments over the timing of the initiation of plate tectonics on Earth are driven in part by differing interpretations of available spatially and temporally fragmented datasets, and through emphasis on selected data that are considered to support a particular outcome. On the modern Earth, features indicative of plate tectonics are directly observable within an established kinematic reference frame and demonstrate lateral movement of rigid plates of oceanic and continental lithosphere about Euler poles of rotation. On the early Earth, or indeed for much of the Palaeozoic and older Earth, the kinematic reference frame is lacking and oceanic lithosphere, which forms some 60% of the present-day surface, is largely lost and limited to rock associations such as ophiolites, which are themselves the source of debate as to their exact tectonic setting (compare [166,216–218]). Furthermore, interpretations of datasets are often disputed; for example, geodynamic setting derived from geochemical signatures. Thus, to date, no individual observation, or even groups of observations, provides unique undisputed evidence for plate tectonics on the early Earth, and it may be that such information is not readily preserved in the geological record. Although evidence from sedimentary, igneous and metamorphic rock associations outlined here can be related to interactions across plate boundaries, some researchers have argued that in the Archaean such features form through lithospheric movement coupled to a convecting mantle, and are not formed by a linked system of plates moving in response to ridge push or slab pull (e.g. [9]).

Our approach is to combine abductive reasoning in which we take observations from what are inevitably particular sites in the geological record, with information from more global datasets to integrate information from different scales and seek the simplest and most likely explanation. The well-known example used to illustrate this logical inference is that if something looks like a duck, swims like a duck, and quacks like a duck, then it probably is a duck. Of course, we realize that individual criteria often provide non-unique interpretations (e.g. the bill of a duck and a duck-bill platypus) but spatially and temporally linked sets of observations (bill, web feet, feathers, quaking) reduces possible alternatives. Thus, the similarity between features formed on the present day, plate tectonic Earth and those back to the late Archaean, such as passive margins, foreland basins, compressional linear structures, temporally paired metamorphic belts, and palaeomagnetically constrained relative motion of lithospheric blocks, as well as the temporal continuity of these features across this time period, validates our interpretation that they formed in a mobile lid regime related to plate tectonics. The time at which individual features appear in the geological record vary, and although this in part reflects the vagaries of preservation, they generally start to appear in the Mesoarchaean and are widespread across most cratons by the end of the Neoarchaean. This increasingly widespread distribution through the Archaean, as well as their noted similarity to features observed on a modern day plate tectonic Earth, suggest they are

not isolated features related to non-plate tectonic or episodic plate tectonic processes but record the parturition of a linked system of lithospheric plates.

Recognition of features considered to be characteristic of subduction, whether they be in the Hadean, Archaean or Proterozoic and younger successions, does not directly constrain the start of plate tectonics; subduction does not in and of itself equate to plate tectonics. This is because subduction, at least in earlier parts of Earth history, was likely episodic [213,215,219]. Thus, the key issue in defining the start of plate tectonics is not in establishing when subduction first appeared on Earth, although that is a minimum prerequisite, but rather when convergent along with divergent boundaries delineated the edges of a globally linked system of plates. Unfortunately, this concept of a globally linked system can only be established in the post-Pangaea Earth in which ocean floor is preserved, enabling a kinematic reference frame of plate interaction to be established. Recent attempts have been made at full-plate global palaeogeographic models for pre-Pangaean times [220–223]. Nevertheless, when plate tectonics initiated on a pre-Pangaea Earth cannot be unequivocally proven specific proposals can be falsified [224]. The challenge for those proposing a birthdate for plate tectonics is not more evidence for subduction at specific time or place but rather to show that it was sustained and part of a global system of plate boundary interaction. We consider that the progressive development of geological proxies of rigid lithosphere and for convergent and divergent plate interaction across all the major cratons by the late Archaean is the expression of the formation of such a linked system.

In summary, we consider changes in the behaviour and character of the lithosphere in the later parts of the Archaean to be consistent with a gestational transition from a non-plate tectonic mode to the birth of plates, followed by sustained plate tectonics. We emphasize the need to avoid arguments built on observations from specific regions or data types, not least because of the difficulties in establishing the wider significance of localized datasets in highly heterogeneous material, such as the continental crust. Such information is important but it must be part of a multicomponent analysis to build geologically constrained and integrated global datasets. For it is only through the integration of information from different scales that Earth-wide linked evolutionary trends can be established, and those remain the prerequisite in recognizing tectonic modes of lithospheric plate interaction.

Data accessibility. This article has no additional data.

Authors' contributions. P.A.C. and C.J.H. were involved in the overall conception, design and writing of the manuscript. S.A.P. and P.A.C. wrote the section on palaeomagnetics. B.D., F.A.C. and O.N. contributed to the geochemistry and geodynamics sections and linked these to the overall tectonic framework. All authors read and approved the manuscript.

Competing interests. We declare we have no competing interests.

Funding. We acknowledge support from Australian Research Council grant nos. FL160100168, FL150100133, FT170100254 and FT140101062, Leverhulme Trust RPG-2015-422 and EM-2017-047/4, and NERC NE/K008862/1.

Acknowledgements. Our ideas on the how, when, where and why of plate tectonics have evolved over many years and we thank the following for stimulating discussion: Mike Brown, Mike Daly, Tony Kemp, Mike Kendall, Alfred Kroener, Tony Prave, Guochun Zhao. We thank Ginaldo Campanha, Arthur Hickman, Fabian Humbert, Laurence Robb, Michael Wingate, Wei Wang (CUGB), Wei Wang (CUGW) and Ivan Zibra for providing information. Nick Arndt and Tim Kusky provided reviews which helped further clarify our ideas.

References

1. Davies GF. 1999 *Dynamic earth plates, plumes and mantle convection*. Cambridge, UK: Cambridge University Press.
2. Cawood PA, Kröner A, Pisarevsky S. 2006 Precambrian plate tectonics: criteria and evidence. *GSA Today* **16**, 4–11. (doi:10.1130/GSAT01607.1)
3. Stern RJ. 2005 Evidence from ophiolites, blueschists, and ultrahigh-pressure metamorphic terranes that the modern episode of subduction tectonics began in Neoproterozoic time. *Geology* **33**, 557–560. (doi:10.1130/g21365.1)

4. Hopkins MD, Harrison TM, Manning CE. 2010 Constraints on Hadean geodynamics from mineral inclusions in >4 Ga zircons. *Earth Planet. Sci. Lett.* **298**, 367–376. (doi:10.1016/j.epsl.2010.08.010)
5. Korenaga J. 2013 Initiation and evolution of plate tectonics on earth: theories and observations. *Ann. Rev. Earth Planet. Sci.* **41**, 117–151. (doi:10.1146/annurev-earth-050212-124208)
6. Lenardic A. 2018 The diversity of tectonic modes and thoughts about transitions between them. *Phil. Trans. R. Soc. A* **376**, 20170416. (doi:10.1098/rsta.2017.0416)
7. Solomatov VS, Moresi LN. 1997 Three regimes of mantle convection with non-Newtonian viscosity and stagnant lid convection on the terrestrial planets. *Geophys. Res. Lett.* **24**, 1907–1910. (doi:10.1029/97GL01682)
8. Gerya T. 2014 Precambrian geodynamics: concepts and models. *Gondwana Res.* **25**, 442–463. (doi:10.1016/j.gr.2012.11.008)
9. Bédard JH. 2018 Stagnant lids and mantle overturns: implications for Archaean tectonics, magmagenesis, crustal growth, mantle evolution, and the start of plate tectonics. *Geosci. Front.* **9**, 19–49. (doi:10.1016/j.gsf.2017.01.005)
10. Griffin WL, Belousova EA, O'Neill C, O'Reilly SY, Malkovets V, Pearson NJ, Spetsius S, Wilde SA. 2014 The world turns over: Hadean–Archean crust–mantle evolution. *Lithos* **189**, 2–15. (doi:10.1016/j.lithos.2013.08.018)
11. Amante C, Eakins BW. 2009 *ETOPO1 1 Arc-Minute Global Relief Model: Procedures, Data Sources and Analysis*, p. 25. NOAA Technical Memorandum NESDIS NGDC-24 ed. Boulder, Colorado: National Ocean and Atmospheric Administration.
12. Cooper CM, Miller MS, Moresi L. 2017 The structural evolution of the deep continental lithosphere. *Tectonophysics* **695**, 100–121. (doi:10.1016/j.tecto.2016.12.004)
13. Cogley JG. 1984 Continental margins and the extent and number of the continents. *Rev. Geophys.* **22**, 101–122. (doi:10.1029/RG022i002p00101)
14. Forsyth D, Uyeda S. 1975 On the relative importance of the driving forces of plate motion. *Geophys. J. R. Astron. Soc.* **43**, 163–200. (doi:10.1111/j.1365-246X.1975.tb00631.x)
15. Cloos M. 1993 Lithospheric buoyancy and collisional orogenesis: subduction of oceanic plateaus, continental margins, island arcs, spreading ridges, and seamounts. *Geol. Soc. Am. Bull.* **105**, 715–737. (doi:10.1130/0016-7606(1993)105<0715:lbacos>2.3.co;2)
16. Stern RJ. 2002 Subduction zones. *Rev. Geophys.* **40**, 3-1–3-38. (doi:10.1029/2001RG000108)
17. Ringwood AE. 1974 The petrological evolution of island arc systems. *J. Geol. Soc.* **130**, 183–204. (doi:10.1144/gsjgs.130.3.0183)
18. Gill JB. 1981 *Orogenic Andesites and plate tectonics*. Berlin, Germany: Springer.
19. Cawood PA, Hawkesworth CJ, Dhuime B. 2013 The continental record and the generation of continental crust. *Geol. Soc. Am. Bull.* **125**, 14–32. (doi:10.1130/b30722.1)
20. Taylor SR. 1967 The origin and growth of continents. *Tectonophysics* **4**, 17–34. (doi:10.1016/0040-1951(67)90056-X)
21. Rudnick RL, Gao S. 2003 Composition of the continental crust. In *Treatise on geochemistry, vol. 3, The crust* (ed. RL Rudnick), p. 64. Amsterdam, The Netherlands: Elsevier.
22. Moresi L, Solomatov V. 1998 Mantle convection with a brittle lithosphere: thoughts on the global tectonic styles of the Earth and Venus. *Geophys. J. Int.* **133**, 669–682. (doi:10.1046/j.1365-246X.1998.00521.x)
23. Sizova E, Gerya T, Brown M, Perchuk LL. 2010 Subduction styles in the Precambrian: insight from numerical experiments. *Lithos* **116**, 209–229. (doi:10.1016/j.lithos.2009.05.028)
24. Tackley PJ. 1998 Self-consistent generation of tectonic plates in three-dimensional mantle convection. *Earth Planet. Sci. Lett.* **157**, 9–22. (doi:10.1016/S0012-821X(98)00029-6)
25. Fedo CM, Eriksson KA. 1994 Archean Synrift and Stable-Shelf Sedimentary Successions. In *Developments in precambrian geology* (ed. KC Condie), pp. 171–204. Amsterdam, The Netherlands: Elsevier.
26. Allen PA, Eriksson PG, Alkmim FF, Betts PG, Catuneanu O, Mazumder R, Meng Q, Young GM. 2015 Chapter 2 Classification of basins, with special reference to proterozoic examples. *Geolog. Soc. Lond. Mem.* **43**, 5–28. (doi:10.1144/m43.2)
27. Evans DAD, Pisarevsky SA. 2008 Plate tectonics on early Earth? Weighing the paleomagnetic evidence. In *When did plate tectonics begin on planet earth?* (eds KC Condie, V Pease), pp. 249–263. Boulder, CO: Geological Society of America.

28. Ernst RE. 2014 *Large igneous provinces*, 1–653 p. Cambrdige, UK: Cambridge University Press.
29. Zeh A, Wilson AH, Ovtcharova M. 2016 Source and age of upper Transvaal supergroup, South Africa: age-Hf isotope record of zircons in Magaliesberg quartzite and Dullstroom lava, and implications for paleoproterozoic (2.5–2.0 Ga) continent reconstruction. *Precambrian Res.* **278**, 1–21. (doi:10.1016/j.precamres.2016.03.017)
30. Eriksson PG, Altermann W, Catuneanu O, van der Merwe R, Bumby AJ. 2001 Major influences on the evolution of the 2.67–2.1 Ga Transvaal basin, Kaapvaal craton. *Sediment. Geol.* **141–142**, 205–231. (doi:10.1016/S0037-0738(01)00075-6)
31. Arndt NT, Nelson DR, Compston W, Trendall AF, Thorne AM. 1991 The age of the Fortescue Group, Hamersley Basin, Western Australia, from ion microprobe zircon U-Pb results. *Aust. J. Earth Sci.* **38**, 261–281. (doi:10.1080/08120099108727971)
32. Müller SG, Krapež B, Barley ME, Fletcher IR. 2005 Giant iron-ore deposits of the Hamersley province related to the breakup of Paleoproterozoic Australia: new insights from in situ SHRIMP dating of baddeleyite from mafic intrusions. *Geology* **33**, 577–580. (doi:10.1130/G21482.1)
33. Siahi M, Hofmann A, Hegner E, Master S. 2016 Sedimentology and facies analysis of Mesoarchaean stromatolitic carbonate rocks of the Pongola Supergroup, South Africa. *Precambrian Res.* **278**, 244–264. (doi:10.1016/j.precamres.2016.03.004)
34. Catuneanu O. 2001 Flexural partitioning of the Late Archaean Witwatersrand foreland system, South Africa. *Sediment. Geol.* **141–142**, 95–112. (doi:10.1016/S0037-0738(01)00070-7)
35. Heubeck C, Engelhardt J, Byerly GR, Zeh A, Sell B, Luber T, Lowe DR. 2013 Timing of deposition and deformation of the Moodies Group (Barberton Greenstone Belt, South Africa): very-high-resolution of Archaean surface processes. *Precambrian Res.* **231**, 236–262. (doi:10.1016/j.precamres.2013.03.021)
36. Burke K, Kidd WSF, Kusky T. 1985 Is the Ventersdorp Rift System of Southern Africa related to a continental collision between the Kaapvaal and Zimbabwe Cratons at 2.64 Ga ago? *Tectonophysics* **115**, 1–24. (doi:10.1016/0040-1951(85)90096-4)
37. Burke K, Kidd WSF, Kusky TM. 1985 The Pongola structure of southeastern Africa: the world's oldest preserved rift? *J. Geodyn.* **2**, 35–49. (doi:10.1016/0264-3707(85)90031-6)
38. Burke K, Kidd WSF, Kusky TM. 1986 Archean Foreland Basin tectonics in the Witwatersrand, South Africa. *Tectonics* **5**, 439–456. (doi:10.1029/TC005i003p00439)
39. Srinivasan R, Ojakangas RW. 1986 Sedimentology of Quartz-Pebble Conglomerates and Quartzites of the Archean Bababudan Group, Dharwar Craton, South India: evidence for Early Crustal Stability. *J. Geol.* **94**, 199–214. (doi:10.1086/629023)
40. Bekker A, Sial AN, Karhu JA, Ferreira VP, Noce CM, Kaufman AJ, Romano AW, Pimentel MM. 2003 Chemostratigraphy of carbonates from the Minas Supergroup, Quadrilátero Ferryífero (Iron Quadrangle), Brazil: a stratigraphic record of early proterozoic atmospheric, biogeochemical and climactic change. *Am. J. Sci.* **303**, 865–904. (doi:10.2475/ajs.303.10.865)
41. Young GM, Long DGF, Fedo CM, Nesbitt HW. 2001 Paleoproterozoic Huronian basin: product of a Wilson cycle punctuated by glaciations and a meteorite impact. *Sediment. Geol.* **141–142**, 233–254. (doi:10.1016/S0037-0738(01)00076-8)
42. Ojakangas RW, Marmo JS, Heiskanen KI. 2001 Basin evolution of the Paleoproterozoic Karelian Supergroup of the Fennoscandian (Baltic) shield. *Sediment. Geol.* **141–142**, 255–285. (doi:10.1016/S0037-0738(01)00079-3)
43. Wang W, Cawood PA, Pandit MK, Zhou M-F, Chen W-T. 2017 Zircon U–Pb age and Hf isotope evidence for an Eoarchaean crustal remnant and episodic crustal reworking in response to supercontinent cycles in NW India. *J. Geol. Soc.* **174**, 759–772. (doi:10.1144/jgs2016-080)
44. Nutman AP, Friend CRL, Bennett VC, McGregor VR. 2004 Dating of the Ameralik dyke swarms of the Nuuk district, southern West Greenland: mafic intrusion events starting from c. 3510 Ma. *J. Geol. Soc.* **161**, 421–430. (doi:10.1144/0016-764903-043)
45. Gill RCO, Bridgwater D. 1976 The Ameralik dykes of West Greenland, the earliest known basaltic rocks intruding stable continental crust. *Earth Planet. Sci. Lett.* **29**, 276–282. (doi:10.1016/0012-821X(76)90131-X)
46. Wilson AH, Zeh A. 2018 U-Pb and Hf isotopes of detrital zircons from the Pongola Supergroup: constraints on deposition ages, provenance and Archean evolution of the Kaapvaal craton. *Precambrian Res.* **305**, 177–196. (doi:10.1016/j.precamres.2017.12.020)

47. Wingate MTD. 1999 Ion microprobe baddeleyite and zircon ages for Late Archaean mafic dykes of the Pilbara Craton, Western Australia. *Aust. J. Earth Sci.* **46**, 493–500. (doi:10.1046/j.1440-0952.1999.00726.x)
48. Wingate MTD, Lu Y, Johnson SP. 2017 205904: metagabbro dyke, Black Hill Bore. In *Geochronology record 1365*, p. 4. Perth, Australia: Geological Survey of Western Australia.
49. Oberthür T, Davis DW, Blenkinsop TG, Höhndorf A. 2002 Precise U–Pb mineral ages, Rb–Sr and Sm–Nd systematics for the Great Dyke, Zimbabwe—constraints on late Archean events in the Zimbabwe craton and Limpopo belt. *Precambrian Res.* **113**, 293–305. (doi:10.1016/S0301-9268(01)00215-7)
50. Söderlund U, Hofmann A, Klausen MB, Olsson JR, Ernst RE, Persson P-O. 2010 Towards a complete magmatic barcode for the Zimbabwe craton: Baddeleyite U–Pb dating of regional dolerite dyke swarms and sill complexes. *Precambrian Res.* **183**, 388–398. (doi:10.1016/j.precamres.2009.11.001)
51. Nemchin AA, Pidgeon RT. 1998 Precise conventional and SHRIMP baddeleyite U-Pb age for the Binneringie Dyke, near Narrogin, Western Australia. *Aust. J. Earth Sci.* **45**, 673–675. (doi:10.1080/08120099808728424)
52. Krogh TE. 1994 Precise U-Pb ages for Grenvillian and pre-Grenvillian thrusting of Proterozoic and Archean metamorphic assemblages in the Grenville Front tectonic zone, Canada. *Tectonics* **13**, 963–982. (doi:10.1029/94TC00801)
53. Kumar A, Hamilton MA, Halls HC. 2012 A Paleoproterozoic giant radiating dyke swarm in the Dharwar Craton, southern India. *Geochem. Geophys. Geosyst.* **13**. (doi:10.1029/2011GC003926)
54. Bleeker W, Ernst RE. 2006 Short-lived mantle generated magmatic events and their dike swarms: the key unlocking Earth's paleogeographic record back to 2.6 Ga. In *Dike swarms: time markers of crustal evolution* (eds E Hanski, S Mertanen, T Rämö, J Vuollo), pp. 3–26. Leiden, The Netherlands: Taylor & Francis/Balkema.
55. Artemieva IM, Mooney WD. 2001 Thermal thickness and evolution of Precambrian lithosphere: a global study. *J. Geophys. Res. Solid Earth (1978–2012)* **106**, 16 387–16 414. (doi:10.1029/2000JB900439)
56. Durrheim RJ, Mooney WD. 1991 Archean and Proterozoic crustal evolution: evidence from crustal seismology. *Geology* **19**, 606–609. (doi:10.1130/0091-7613(1991)019<0606:AAPCEE>2.3.CO;2)
57. Armstrong RL. 1981 Radiogenic Isotopes: the case for crustal recycling on a near-steady-state no-continental-growth earth. *Phil. Trans. R. Soc. A* **301**, 443–472. (doi:10.1098/rsta.1981.0122)
58. Begg GC *et al.* 2009 The lithospheric architecture of Africa: Seismic tomography, mantle petrology, and tectonic evolution. *Geosphere* **5**, 23–50. (doi:10.1130/ges00179.1)
59. Laurent O, Martin H, Moyen JF, Doucelance R. 2014 The diversity and evolution of late-Archean granitoids: evidence for the onset of 'modern-style' plate tectonics between 3.0 and 2.5 Ga. *Lithos* **205**, 208–235. (doi:10.1016/j.lithos.2014.06.012)
60. Wang W, Cawood PA, Liu S, Guo R, Bai X, Wang K. 2017 Cyclic formation and stabilization of Archean lithosphere by accretionary orogenesis: constraints from TTG and potassic granitoids, North China Craton. *Tectonics* **36**, 1724–1742. (doi:10.1002/2017TC004600)
61. Nebel O, Capitanio F, Moyen J-F, Weinberg R, Clos F, Nebel-Jacobsen YJ, Cawood PA. 2018 When crust comes of age: on the chemical evolution of Archaean, felsic continental crust by crustal drip tectonics. *Phil. Trans. R. Soc. A* **376**, 20180103. (doi:10.1098/rsta.2018.0103)
62. Bose PK, Eriksson PG, Sarkar S, Wright DT, Samanta P, Mukhopadhyay S, Mandal S, Banerjee S, Altermann W. 2012 Sedimentation patterns during the Precambrian: a unique record? *Mar. Pet. Geol.* **33**, 34–68. (doi:10.1016/j.marpetgeo.2010.11.002)
63. Eriksson PG *et al.* 2013 Secular changes in sedimentation systems and sequence stratigraphy. *Gondwana Res.* **24**, 468–489. (doi:10.1016/j.gr.2012.09.008)
64. Brown M, Johnson T. 2018 Secular change in metamorphism and the onset of global plate tectonics. *Am. Mineral.* **103**, 181–196. (doi:10.2138/am-2018-6166)
65. Keller B, Schoene B. 2018 Plate tectonics and continental basaltic geochemistry throughout Earth history. *Earth Planet. Sci. Lett.* **481**, 290–304. (doi:10.1016/j.epsl.2017.10.031)
66. Ingersoll RV. 2012 Tectonics of sedimentary basins, with revised nomenclature. In *Tectonics of sedimentary basins: recent advances* (eds CJ Busby, A Azor), pp. 3–43. Oxford, UK: Blackwell Publishing Ltd.

67. Bradley DC. 2008 Passive margins through earth history. *Earth Sci. Rev.* **91**, 1–26. (doi:10.1016/j.earscirev.2008.08.001)
68. Cawood PA, McCausland PJA, Dunning GR. 2001 Opening Iapetus: constraints from the Laurentian margin in Newfoundland. *Geol. Soc. Am. Bull.* **113**, 443–453. (doi:10.1130/0016-7606(2001)113<0443:OICFTL>2.0.CO;2)
69. Cawood PA, Nemchin AA. 2001 Source regions for Laurentian margin sediments: constraints from U/Pb dating of detrital zircon in the Newfoundland Appalachians. *Geol. Soc. Am. Bull.* **113**, 1234–1246. (doi:10.1130/0016-7606(2001)113<1234:PDOTEL>2.0.CO;2)
70. Corcoran PL, Mueller WU. 2004 Archaean Sedimentary Sequences. In *The precambrian events: tempos and events* (eds PG Eriksson, W Altermann, DR Nelson, WU Mueller, O Catuneanu), pp. 613–624. Amsterdam, The Netherlands: Elsevier.
71. Blake TS, Barley ME. 1992 Tectonic evolution of the Late Archaean to Early Proterozoic Mount Bruce Megasequence Set, western Australia. *Tectonics* **11**, 1415–1425. (doi:10.1029/92TC00339)
72. Martin DM, Clendenin CW, Krapez B, McNaughton NJ. 1998 Tectonic and geochronological constraints on late Archaean and Palaeoproterozoic stratigraphic correlation within and between the Kaapvaal and Pilbara Cratons. *J. Geol. Soc.* **155**, 311–322. (doi:10.1144/gsjgs.155.2.0311)
73. Hofmann A, Kusky T. 2004 The Belingwe Greenstone Belt: Ensialic or Oceanic? In *Developments in precambrian geology*, pp. 487–538. Amsterdam, The Netherlands: Elsevier.
74. Zhao G, Sun M, Wilde SA, Sanzhong L. 2005 Late Archean to Paleoproterozoic evolution of the North China Craton: key issues revisited. *Precambrian Res.* **136**, 177–202. (doi:10.1016/j.precamres.2004.10.002)
75. Kusky TM, Li J. 2003 Paleoproterozoic tectonic evolution of the North China Craton. *J. Asian Earth Sci.* **22**, 383–397. (doi:10.1016/S1367-9120(03)00071-3)
76. Beukes NJ. 1984 Sedimentology of the Kuruman and Griquatown Iron-formations, Transvaal Supergroup, Griqualand West, South Africa. *Precambrian Res.* **24**, 47–84. (doi:10.1016/0301-9268(84)90069-X)
77. Blake TS. 1993 Late Archaean crustal extension, sedimentary basin formation, flood basalt volcanism and continental rifting: the Nullagine and Mt Jope supersequences, Western Australia. *Precambrian Res.* **60**, 185–241. (doi:10.1016/0301-9268(93)90050-C)
78. Blake TS. 2001 Cyclic continental mafic tuff and flood basalt volcanism in the Late Archaean Nullagine and Mount Jope Supersequences in the eastern Pilbara, Western Australia. *Precambrian Res.* **107**, 139–177. (doi:10.1016/S0301-9268(00)00135-2)
79. Dhuime B, Hawkesworth CJ, Cawood PA, Storey CD. 2012 A change in the geodynamics of continental growth 3 billion years ago. *Science* **335**, 1334–1336. (doi:10.1126/science.1216066)
80. Dhuime B, Wuestefeld A, Hawkesworth CJ. 2015 Emergence of modern continental crust about 3 billion years ago. *Nat. Geosci.* **8**, 552–555. (doi:10.1038/ngeo2466)
81. Spencer CJ, Cawood PA, Hawkesworth CJ, Raub TD, Prave AR, Roberts NMW. 2014 Proterozoic onset of crustal reworking and collisional tectonics: reappraisal of the zircon oxygen isotope record. *Geology* **42**, 451–454. (doi:10.1130/g35363.1)
82. Shields GA. 2007 A normalised seawater strontium isotope curve: possible implications for Neoproterozoic-Cambrian weathering rates and the further oxygenation of the Earth. *eEarth* **2**, 35–42. (doi:10.5194/ee-2-35-2007)
83. Satkoski AM, Fralick P, Beard BL, Johnson CM. 2017 Initiation of modern-style plate tectonics recorded in Mesoarchean marine chemical sediments. *Geochim. Cosmochim. Acta* **209**, 216–232. (doi:10.1016/j.gca.2017.04.024)
84. Satkoski AM, Lowe DR, Beard BL, Coleman ML, Johnson CM. 2016 A high continental weathering flux into Paleoarchean seawater revealed by strontium isotope analysis of 3.26 Ga barite. *Earth Planet. Sci. Lett.* **454**, 28–35. (doi:10.1016/j.epsl.2016.08.032)
85. Kusky TM, Hudleston PJ. 1999 Growth and demise of an Archean carbonate platform, Steep Rock Lake, Ontario, Canada. *Can. J. Earth Sci.* **36**, 565–584. (doi:10.1139/e98-108)
86. Woolley AR, Kjarsgaard BA. 2008 Carbonatite occurrences of the world: map and database. (Ottawa, Geological Survey of Canada Open File 5796, 1 CD-ROM + 1 map.
87. Cawood PA, Hawkesworth CJ. 2014 Earth's middle age. *Geology* **42**, 503–506. (doi:10.1130/g35402.1)

88. Hawkesworth C, Cawood P, Kemp T, Storey C, Dhuime B. 2009 A matter of preservation. *Science* **323**, 49–50. (doi:10.1126/science.1168549)
89. Cawood PA, Kröner A, Collins WJ, Kusky TM, Mooney WD, Windley BF. 2009 Accretionary Orogens through Earth History. In *Earth accretionary systems in space and time* (eds PA Cawood, A Kröner), pp. 1–36 (special publication 318). London, UK: Geological Society.
90. Windley BF. 1992 Proterozoic collisional and accretionary orogens. In *Proterozoic crustal evolution* (ed. KC Condie), pp. 419–446. Amsterdam, The Netherlands: Elsevier.
91. Jordan TE. 1995 Retroarc Foreland and Related Basins. In *Tectonics of sedimentary basins* (eds CJ Busby, RV Ingersoll), pp. 331–362. Cambridge, MA: Blackwell Science.
92. Miall AD. 1995 Collision-Related Foreland Basins. In *Tectonics of sedimentary basins* (eds CJ Busby, RV Ingersoll), pp. 393–424. Cambridge, MA: Blackwell Science.
93. Hofmann A, Dirks PHGM, Jelsma HA. 2001 Late Archaean foreland basin deposits, Belingwe greenstone belt, Zimbabwe. *Sediment. Geol.* **141–142**, 131–168. (doi:10.1016/S0037-0738(01)00072-0)
94. Camiré GE, Burg JP. 1993 Late Archaean thrusting in the northwestern Pontiac Subprovince, Canadian Shield. *Precambrian Res.* **61**, 51–66. (doi:10.1016/0301-9268(93)90057-9)
95. Corcoran PL, Mueller WU. 2007 Time-transgressive Archean unconformities underlying Molasse Basin-fill successions of dissected oceanic arcs, superior province, Canada. *J. Geol.* **115**, 655–674. (doi:10.1086/521609)
96. Miall AD, Catuneanu O, Eriksson PG, Mazumder R. 2015 Chapter 23 a brief synthesis of Indian Precambrian basins: classification and genesis of basin-fills. *Geolo. Soc. Lond Mem.* **43**, 339–347. (doi:10.1144/m43.23)
97. Ernst WG. 1972 Occurrence and mineralogic evolution of blueschist belts with time. *Am. J. Sci.* **272**, 657–668. (doi:10.2475/ajs.272.7.657)
98. Glassley WE, Korstgård JA, Ensen KS, Platou SW. 2014 A new UHP metamorphic complex in the ~1.8 Ga Nagssugtoqidian Orogen of west Greenland. *Am. Mineral.* **99**, 1315–1334. (doi:10.2138/am.2014.4726)
99. Weller OM, St-Onge MR. 2017 Record of modern-style plate tectonics in the Palaeoproterozoic Trans-Hudson orogen. *Nat. Geosci.* **10**, 305–311. (doi:10.1038/ngeo2904)
100. Ganne J *et al.* 2012 Modern-style plate subduction preserved in the Palaeoproterozoic West African craton. *Nat. Geosci.* **5**, 60–65. (doi:10.1038/ngeo1321)
101. Carlson WD, Anderson SD, Mosher S, Davidow JS, Crawford WD, Lane ED. 2007 High-pressure metamorphism in the Texas Grenville Oregon: mesoproterozoic subduction of the southern Laurentian continental margin. *Int. Geol. Rev.* **49**, 99–119. (doi:10.2747/0020-6814.49.2.99)
102. Hyndman RD, Currie CA, Mazzotti SP. 2005 Subduction zone backarcs, mobile belts and orogenic heat. *GSA Today* **15**, 4–10. (doi:10.1130/1052-5173(2005)015<4:SZBMBA>2.0.CO;2)
103. Stevens G, Moyen JF. 2007 Metamorphism in the Barberton Granite Greenstone Terrain: A Record of Paleoarchean Accretion. In *Developments in precambrian geology* pp. 669–698. Amsterdam, The Netherlands: Elsevier.
104. Sizova E, Gerya T, Brown M. 2014 Contrasting styles of Phanerozoic and Precambrian continental collision. *Gondwana Res.* **25**, 522–545. (doi:10.1016/j.gr.2012.12.011)
105. Dewey JF. 1982 Plate tectonics and the evolution of the British Isles. *J. Geol. Soc. Lond.* **139**, 371–412. (doi:10.1144/gsjgs.139.4.0371)
106. Dewey JF, Hempton MR, Kidd WSF, Saroglu F, Şengör AMC. 1986 Shortening of continental lithosphere: the neotectonics of Eastern Anatolia: a young collision zone. *Geol. Soc. Lond. Special Publications* **19**, 1–36. (doi:10.1144/gsl.sp.1986.019.01.01)
107. Champion DC, Cassidy KF. 2007 An overview of the Yilgarn Craton and its crustal evolution. In *Proceedings of Geoconferences (WA) Inc. Kalgoorlie '07 Conference, Kalgoorlie, Western Australia* (eds FP Bierlein, CM Knox-Robinson), pp. 8–14. Canberra, Australia: Geoscience Australia Record.
108. McCuaig TC, Miller J, Beresford S. 2010 *Controls on giant minerals systems in the Yilgarn Craton – a field guide*. Perth, Australia: Geological Survey of Western Australia.
109. de Wit MJ, Ashwal LD. 1997 *Greenstone belts*. Oxford, UK: Oxford University Press.
110. Friend CRL, Nutman AP. 2005 New pieces to the Archaean terrane jigsaw puzzle in the Nuuk region, southern West Greenland: steps in transforming a simple insight into

a complex regional tectonothermal model. *J. Geol. Soc.* **162**, 147–162. (doi:10.1144/0016-764903-161)
111. Windley BF, Garde AA. 2009 Arc-generated blocks with crustal sections in the North Atlantic craton of West Greenland: crustal growth in the Archean with modern analogues. *Earth Sci. Rev.* **93**, 1–30. (doi:10.1016/j.earscirev.2008.12.001)
112. Van Kranendonk MJ. 2004 Preface: Archaean Tectonics 2004: a review. *Precambrian Res.* **131**, 143–151. (doi:10.1016/j.precamres.2003.12.008)
113. Chen SF, Riganti A, Wyche S, Greenfield JE, Nelson DR. 2003 Lithostratigraphy and tectonic evolution of contrasting greenstone successions in the central Yilgarn Craton, Western Australia. *Precambrian Res.* **127**, 249–266. (doi:10.1016/S0301-9268(03)00190-6)
114. Komiya T, Maruyama S, Masuda T, Nobda S, Hayashi M, Okamoto K. 1999 Plate tectonics at 3.8–3.7 Ga: field evidence from the Isua Accretionary Complex, southern West Greenland. *J. Geol.* **107**, 515–554. (doi:10.1086/314371)
115. Wang J, Kusky T, Wang L, Polat A, Deng H, Wang C, Wang S. 2017 Structural relationships along a Neoarchean arc-continent collision zone, North China craton. *Geol. Soc. Am. Bull.* **129**, 59–75. (doi:10.1130/B31479.1)
116. Kusky TM *et al.* 2016 Insights into the tectonic evolution of the North China Craton through comparative tectonic analysis: a record of outward growth of Precambrian continents. *Earth Sci. Rev.* **162**, 387–432. (doi:10.1016/j.earscirev.2016.09.002)
117. Calvert AJ, Ludden JN. 1999 Archean continental assembly in the southeastern Superior Province of Canada. *Tectonics* **18**, 412–429. (doi:10.1029/1999TC900006)
118. Calvert AJ, Sawyer EW, Davis WJ, Ludden JN. 1995 Archaean subduction inferred from seismic images of a mantle suture in the Superior Province. *Nature* **375**, 670–674. (doi:10.1038/375670a0)
119. Benn K. 2006 Tectonic delamination of the lower crust during late Archean collision of the Abitibi-Opatica and Pontiac terranes, superior province, Canada. In *Geophysical Monograph Series*, pp. 267–282. Washington DC, USA: American Geophysical Union Publications.
120. Eskola PE. 1948 The problem of mantled gneiss domes. *Q. J. Geol. Soc.* **104**, 461–476. (doi:10.1144/gsl.jgs.1948.104.01-04.21)
121. Choukroune P, Ludden JN, Chardon D, Calvert AJ, Bouhallier H. 1997 Archaean crustal growth and tectonic processes: a comparison of the Superior Province, Canada and the Dharwar Craton, India. *Geol. Soc. Lond. Special Publications* **121**, 63–98. (doi:10.1144/gsl.sp.1997.121.01.04)
122. MacGregor AM. 1951 Some milestones in the Precambrian of Southern Rhodesia. *Proc. Geol. Soc. South Africa* **54**, 27–71.
123. Collins WJ, Van Kranendonk MJ, Teyssier C. 1998 Partial convective overturn of Archaean crust in the east Pilbara Craton, Western Australia: driving mechanisms and tectonic implications. *J. Struct. Geol.* **20**, 1405–1424. (doi:10.1016/S0191-8141(98)00073-X)
124. Sandiford M, Kranendonk MJV, Bodorkos S. 2004 Conductive incubation and the origin of dome-and-keel structure in Archean granite-greenstone terrains: a model based on the eastern Pilbara Craton, Western Australia. *Tectonics* **23**. (doi:10.1029/2002TC001452)
125. Van Kranendonk MJ, Collins WJ, Hickman A, Pawley MJ. 2004 Critical tests of vertical vs. horizontal tectonic models for the Archaean East Pilbara Granite–Greenstone Terrane, Pilbara Craton, Western Australia. *Precambrian Res.* **131**, 173–211. (doi:10.1016/j.precamres.2003.12.015)
126. Hickman AH. 1983 *Geology of the Pilbara block and its environs*. Government of Western Australia.
127. Hickman AH. 1984 Archaean diapirism in the Pilbara Block, Western Australia. In *Precambrian Tectonics Illustrated*, pp. 113–128. Stuttgart, Germany: E. Schweizerbart'sche Verlagsbuchhandlung.
128. Hickman AH. 2004 Two contrasting granite-greenstone terranes in the Pilbara Craton, Australia: evidence for vertical and horizontal tectonic regimes prior to 2900 Ma. *Precambrian Res.* **131**, 153–172. (doi:10.1016/j.precamres.2003.12.009)
129. Smithies RH, Van Kranendonk MJ, Champion DC. 2007 The Mesoarchean emergence of modern-style subduction. *Gondwana Res.* **11**, 50–68. (doi:10.1016/j.gr.2006.02.001)
130. Chardon D, Jayananda M, Peucat J-J. 2011 Lateral constrictional flow of hot orogenic crust: insights from the Neoarchean of south India, geological and geophysical implications for orogenic plateaux. *Geochem. Geophys. Geosyst.* **12**. (doi:10.1029/2010GC003398)

131. Bouhallier H, Chardon D, Choukroune P. 1995 Strain patterns in Archaean dome-and-basin structures: the Dharwar craton (Karnataka, South India). *Earth Planet. Sci. Lett.* **135**, 57–75. (doi:10.1016/0012-821X(95)00144-2)
132. Chardon D, Peucat J-J, Jayananda M, Choukroune P, Fanning CM. 2002 Archean granite-greenstone tectonics at Kolar (South India): interplay of diapirism and bulk inhomogeneous contraction during juvenile magmatic accretion. *Tectonics* **21**, 7-1–7-17. (doi:10.1029/2001TC901032)
133. Chardon D, Jayananda M, Chetty TRK, Peucat JJ. 2008 Precambrian continental strain and shear zone patterns: South Indian case. *J. Geophys. Res. Solid Earth* **113**. (doi:10.1029/2007JB005299)
134. Chardon D, Jayananda M. 2008 Three-dimensional field perspective on deformation, flow, and growth of the lower continental crust (Dharwar craton. India). *Tectonics* **27**. (doi:10.1029/2007TC002120)
135. Bhushan SK, Sahoo P. 2010 Geochemistry of clastic sediments from Sargur supracrustals and Bababudan group, Karnataka: implications on Archaean Proterozoic Boundary. *J. Geol. Soc. India* **75**, 829–840. (doi:10.1007/s12594-010-0068-y)
136. Zibra I, Peternell M, Schiller M, Wingate MTD, Lu Y, Clos F. 2018 Tectono-magmatic evolution of the Neoarchean Yalgoo Dome (Yilgarn Craton): Diapirism in a Pre-Orogenic Setting, Report 176, p. 47. Perth, Western Australia: Geological Survey of Western Australia.
137. Zhao G, Cawood PA. 2012 Precambrian geology of China. *Precambrian Res.* **222–223**, 13–54. (doi:10.1016/j.precamres.2012.09.017)
138. Zhao G, Cawood PA, Li S, Wilde SA, Sun M, Zhang J, He Y, Yin C. 2012 Amalgamation of the North China Craton: key issues and discussion. *Precambrian Res.* **222–223**, 55–76. (doi:10.1016/j.precamres.2012.09.016)
139. Li J, Liu Y-J, Jin W, Li X-H, Neubauer F, Li W-M, Liang C-Y, Wen Q-B, Zhang Y-Y. 2017 Neoarchean tectonics: insight from the Baijiafen ductile shear zone, eastern Anshan, Liaoning Province, NE China. *J. Asian Earth Sci.* **139**, 165–182. (doi:10.1016/j.jseaes.2017.01.019)
140. Liu B, Neubauer F, Liu J, Jin W, Li W, Liang C. 2017 Neoarchean ductile deformation of the Northeastern North China Craton: the Shuangshanzi ductile shear zone in Qinglong, eastern Hebei, North China. *J. Asian Earth Sci.* **139**, 224–236. (doi:10.1016/j.jseaes.2017.01.014)
141. Pearce JA. 2008 Geochemical fingerprinting of oceanic basalts with applications to ophiolite classification and the search for Archean oceanic crust. *Lithos* **100**, 14–48. (doi:10.1016/j.lithos.2007.06.016)
142. Pearce JA, Cann JR. 1973 Tectonic setting of basic volcanic rocks determined using trace element analyses. *Earth Planet. Sci. Lett.* **19**, 290–300. (doi:10.1016/0012-821x(73)90129-5)
143. Polat A. 2012 Growth of Archean continental crust in oceanic island arcs. *Geology* **40**, 383–384. (doi:10.1130/focus042012.1)
144. Polat A, Kerrich R. 2004 Precambrian arc associations: Boninites, adakites, magnesian andesites, and Nb-enriched basalts. In *Precambrian ophiolites and related rocks* (ed. TM Kusky), pp. 567–597. Amsterdam, The Netherlands: Elsevier.
145. Bédard JH. 2006 A catalytic delamination-driven model for coupled genesis of Archaean crust and sub-continental lithospheric mantle. *Geochim. Cosmochim. Acta* **70**, 1188–1214. (doi:10.1016/j.gca.2005.11.008)
146. Bédard JH. 2013 How many arcs can dance on the head of a plume? A 'Comment' on: A critical assessment of Neoarchean 'plume only' geodynamics: evidence from the Superior province, by Derek Wyman, Precambrian Research, 2012. *Precambrian Res.* **229**, 189–197. (doi:10.1016/j.precamres.2012.05.004)
147. Wyman DA. 2013 A critical assessment of Neoarchean 'plume only' geodynamics: evidence from the Superior Province. *Precambrian Res.* **229**, 3–19. (doi:10.1016/j.precamres.2012.01.010)
148. Moyen J-F, Laurent O. 2018 Archaean tectonic systems: a view from igneous rocks. *Lithos* **302–303**, 99–125. (doi:10.1016/j.lithos.2017.11.038)
149. Cameron WE, Nisbet EG, Dietrich VJ. 1980 Boninites, komatiites and ophiolitic basalts. *Nature* **280**, 550–553. (doi:10.1038/280550a0)
150. Smithies RH, Champion DC, Sun S-S. 2004 The case for Archean boninites. *Contrib. Mineral. Petrol.* **147**, 705–721. (doi:10.1007/s00410-004-0579-x)

151. Kerrich R, Wyman D, Fan J, Bleeker W. 1998 Boninite series: low Ti-tholeiite associations from the 2.7 Ga Abitibi greenstone belt. *Earth Planet. Sci. Lett.* **164**, 303–316. (doi:10.1016/S0012-821X(98)00223-4)
152. Turner S, Rushmer T, Reagan M, Moyen J-F. 2014 Heading down early on? Start of subduction on Earth. *Geology* **42**, 139–142. (doi:10.1130/g34886.1)
153. Dhuime B, Hawkesworth CJ, Delavault H, Cawood PA. 2018 Rates of generation and destruction of the continental crust: implications for continental growth. *Phil. Trans. R. Soc. A* **376**, 20170403. (doi:10.1098/rsta.2017.0403)
154. Barley ME, Loader SE, McNaughton NJ. 1998 3430 to 3417 Ma calc-alkaline volcanism in the McPhee Dome and Kelley Belt, and growth of the eastern Pilbara Craton. *Precambrian Res.* **88**, 3–24. (doi:10.1016/S0301-9268(97)00061-2)
155. Smithies RH, Champion DC, Van Kranendonk MJ. 2005 Modern-style subduction processes in the Mesoarchean: geochemical evidence from the 3.12 Ga Whundo intra-oceanic arc. *Earth Planet. Sci. Lett.* **231**, 221–237. (doi:10.1016/j.epsl.2004.12.026)
156. O'Neil J, Mauruce C, Stevensn RK, Larocque J, Cloquet C, David J, Francis D. 2007 The Geology of the 3.8 Ga Nuvvuagittuq (Porpoise Cove) Greenstone Belt, Northeastern Superior Province, Canada. In *Earth's oldest rocks* (eds MJ van Kranendonk, H Smithies, VC Bennett), pp. 219–254. Amsterdam, The Netherlands: Elsevier.
157. Jenner FE, Bennett VC, Nutman AP, Friend CRL, Norman MD, Yaxley G. 2009 Evidence for subduction at 3.8 Ga: geochemistry of arc-like metabasalts from the southern edge of the Isua Supracrustal Belt. *Chem. Geol.* **261**, 82–97. (doi:10.1016/j.chemgeo.2008.09.016)
158. Jenner FE, Bennett VC, Yaxley G, Friend CRL, Nebel O. 2013 Eoarchean within-plate basalts from southwest Greenland. *Geology* **41**, 327–330. (doi:10.1130/g33787.1)
159. Puchtel IS, Blichert-Toft J, Touboul M, Walker RJ, Byerly GR, Nisbet EG, Anhaeusser CR. 2013 Insights into early Earth from Barberton komatiites: evidence from lithophile isotope and trace element systematics. *Geochim. Cosmochim. Acta* **108**, 63–90. (doi:10.1016/j.gca.2013.01.016)
160. Shimizu K, Nakamura E, Maruyama S. 2005 The Geochemistry of Ultramafic to Mafic Volcanics from the Belingwe Greenstone Belt, Zimbabwe: magmatism in an Archean Continental Large Igneous Province. *J. Petrol.* **46**, 2367–2394. (doi:10.1093/petrology/egi059)
161. de Joux A, Thordarson T, Fitton JG, Hastie AR. 2014 The Cosmos greenstone succession, Agnew-Wiluna greenstone belt, Yilgarn Craton, Western Australia: geochemistry of an enriched Neoarchaean volcanic arc succession. *Lithos* **205**, 148–167. (doi:10.1016/j.lithos.2014.06.013)
162. Polat A, Appel PWU, Fryer BJ. 2011 An overview of the geochemistry of Eoarchean to Mesoarchean ultramafic to mafic volcanic rocks, SW Greenland: implications for mantle depletion and petrogenetic processes at subduction zones in the early Earth. *Gondwana Res.* **20**, 255–283. (doi:10.1016/j.gr.2011.01.007)
163. Polat A, Hofmann AW, Rosing MT. 2002 Boninite-like volcanic rocks in the 3.7–3.8 Ga Isua greenstone belt, West Greenland: geochemical evidence for intra-oceanic subduction zone processes in the early Earth. *Chem. Geol.* **184**, 231–254. (doi:10.1016/S0009–2541(01)00363-1)
164. Smithies RH, Van Kranendonk MJ, Champion DC. 2005 It started with a plume – early Archaean basaltic proto-continental crust. *Earth Planet. Sci. Lett.* **238**, 284–297. (doi:10.1016/j.epsl.2005.07.023)
165. Polat A, Frei R, Longstaffe FJ, Woods R. 2018 Petrogenetic and geodynamic origin of the Neoarchean Doré Lake Complex, Abitibi subprovince, Superior Province, Canada. *Int. J. Earth Sci. (Geol Rundsch)* **107**, 811–843. (doi:10.1007/s00531-017-1498-1)
166. Bédard JH, Harris LB, Thurston PC. 2013 The hunting of the snArc. *Precambrian Res.* **229**, 20–48. (doi:10.1016/j.precamres.2012.04.001)
167. Percival JA, Skulski T, Sanborn-Barrie M, Stott GM, Leclair AD, Corkery MT, Boily M. 2012 Geology and tectonic evolution of the Superior province, Canada. In *Tectonic styles in Canada: the LITHOPROBE perspective* (eds JA Percival. FA Cook, RM Clowes), pp. 321–378. Vancouver, Canada: Geological Association of Canada.
168. Smithies RH, Ivanic TJ, Lowrey JR, Morris PA, Barnes SJ, Wyche S, Lu Y-J. 2018 Two distinct origins for Archean greenstone belts. *Earth Planet. Sci. Lett.* **487**, 106–116. (doi:10.1016/j.epsl.2018.01.034)

169. Wang W, Liu S, Cawood PA, Bai X, Guo R, Guo B, Wang K. 2016 Late Neoarchean subduction-related crustal growth in the Northern Liaoning region of the North China Craton: Evidence from ~2.55 to 2.50 Ga granitoid gneisses. *Precambrian Res.* **281**, 200–223. (doi:10.1016/j.precamres.2016.05.018)
170. Layer PW, Kröner A, McWilliams M, York D. 1989 Elements of the Archean thermal history and apparent polar wander of the eastern Kaapvaal Craton, Swaziland, from single grain dating and paleomagnetism. *Earth Planet. Sci. Lett.* **93**, 23–34. (doi:10.1016/0012-821X(89)90181-7)
171. Evans DA, Beukes NJ, Kirschvink JL. 1997 Low-latitude glaciation in the Palaeoproterozoic era. *Nature* **386**, 262. (doi:10.1038/386262a0)
172. Gumsley AP, Chamberlain KR, Bleeker W, Söderlund U, de Kock MO, Larsson ER, Bekker A. 2017 Timing and tempo of the great oxidation event. *Proc. Natl Acad. Sci. USA* **114**, 1811–1816. (doi:10.1073/pnas.1608824114)
173. Van der Voo R. 1990 The reliability of paleomagnetic data. *Tectonophysics* **184**, 1–9. (doi:10.1016/0040-1951(90)90116-P)
174. Wingate MTD. 1998 A palaeomagnetic test of the Kaapvaal - Pilbara (Vaalbara) connection at 2.78 Ga. *S. Afr. J. Geol.* **101**, 257–274.
175. Evans DAD, Smirnov AV, Gumsley AP. 2017 Paleomagnetism and U–Pb geochronology of the Black Range dykes, Pilbara Craton, Western Australia: a Neoarchean crossing of the polar circle. *Aust. J. Earth Sci.* **64**, 225–237. (doi:10.1080/08120099.2017.1289981)
176. Strik G, de Wit MJ, Langereis CG. 2007 Palaeomagnetism of the Neoarchaean Pongola and Ventersdorp Supergroups and an appraisal of the 3.0–1.9 Ga apparent polar wander path of the Kaapvaal Craton, Southern Africa. *Precambrian Res.* **153**, 96–115. (doi:10.1016/j.precamres.2006.11.006)
177. Strik G, Blake TS, Zegers TE, White SH, Langereis CG. 2003 Palaeomagnetism of flood basalts in the Pilbara Craton, Western Australia: Late Archaean continental drift and the oldest known reversal of the geomagnetic field. *J. Geophys. Res. Solid Earth* **108**, EPM 2-1–EPM 2-21.
178. Pullaiah G, Irving E. 1975 Paleomagnetism of the contact aureole and late dikes of the Otto Stock, Ontario, and its application to Early Proterozoic apparent polar wandering. *Can. J. Earth Sci.* **12**, 1609–1618. (doi:10.1139/e75-143)
179. Mertanen S, Korhonen F. 2011 Paleomagnetic constraints on an Archean-Paleoproterozoic Superior-Karelia connection: New evidence from Archean Karelia. *Precambrian Res.* **186**, 193–204. (doi:10.1016/j.precamres.2011.01.018)
180. Lubnina N, Ernst R, Klausen M, Söderlund U. 2010 Paleomagnetic study of NeoArchean-Paleoproterozoic dykes in the Kaapvaal Craton. *Precambrian Res.* **183**, 523–552. (doi:10.1016/j.precamres.2010.05.005)
181. Evans DAD, Halls HC. 2010 Restoring Proterozoic deformation within the Superior craton. *Precambrian Res.* **183**, 474–489. (doi:10.1016/j.precamres.2010.02.007)
182. Mertanen S, Vuollo JI, Huhma H, Arestova NA, Kovalenko A. 2006 Early Paleoproterozoic-Archean dykes and gneisses in Russian Karelia of the Fennoscandian Shield—New paleomagnetic, isotope age and geochemical investigations. *Precambrian Res.* **144**, 239–260. (doi:10.1016/j.precamres.2005.11.005)
183. Tang M, Chen K, Rudnick RL. 2016 Archean upper crust transition from mafic to felsic marks the onset of plate tectonics. *Science* **351**, 372–375. (doi:10.1126/science.aad5513)
184. Smit MA, Mezger K. 2017 Earth's early O_2 cycle suppressed by primitive continents. *Nat. Geosci.* **10**, 788. (doi:10.1038/ngeo3030)
185. Keller CB, Schoene B. 2012 Statistical geochemistry reveals disruption in secular lithospheric evolution about 2.5 Gyr ago. *Nature* **485**, 490–493. (doi:10.1038/nature11024)
186. Greber ND, Dauphas N, Bekker A, Ptáček MP, Bindeman IN, Hofmann A. 2017 Titanium isotopic evidence for felsic crust and plate tectonics 3.5 billion years ago. *Science* **357**, 1271–1274. (doi:10.1126/science.aan8086)
187. Valley JW *et al.* 2005 4.4 billion years of crustal maturation: oxygen isotope ratios of magmatic zircon. *Contrib. Mineral. Petrol.* **150**, 561–580. (doi:10.1007/s00410-005-0025-8)
188. Shirey SB, Richardson SH. 2011 Start of the Wilson Cycle at 3 Ga Shown by diamonds from Subcontinental Mantle. *Science* **333**, 434–436. (doi:10.1126/science.1206275)
189. Shields G, Veizer J. 2002 Precambrian marine carbonate isotope database: version 1.1. *Geochem. Geophys. Geosyst.* **3**, 1–12. (doi:10.1029/2001GC000266)

190. Pons ML, Fujii T, Rosing M, Quitté G, Télouk P, Albarède F. 2013 A Zn isotope perspective on the rise of continents. *Geobiology* **11**, 201–214. (doi:10.1111/gbi.12030)
191. Viehmann S, Hoffmann JE, Münker C, Bau M. 2014 Decoupled Hf-Nd isotopes in Neoarchean seawater reveal weathering of emerged continents. *Geology* **42**, 115–118. (doi:10.1130/g35014.1)
192. Rey PF, Coltice N. 2008 Neoarchean lithospheric strengthening and the coupling of Earth's geochemical reservoirs. *Geology* **36**, 635–638. (doi:10.1130/g25031a.1;)
193. Campbell IH, Davies DR. 2017 Raising the continental crust. *Earth Planet. Sci. Lett.* **460**, 112–122. (doi:10.1016/j.epsl.2016.12.011)
194. Arndt N. 1999 Why was flood volcanism on submerged continental platforms so common in the Precambrian? *Precambrian Res.* **97**, 155–164. (doi:10.1016/S0301–9268(99)00030–3)
195. Kump LR, Barley ME. 2007 Increased subaerial volcanism and the rise of atmospheric oxygen 2.5[thinsp] billion years ago. *Nature* **448**, 1033–1036. (doi:10.1038/nature06058)
196. Labrosse S, Jaupart C. 2007 Thermal evolution of the Earth: secular changes and fluctuations of plate characteristics. *Earth Planet. Sci. Lett.* **260**, 465–481. (doi:10.1016/j.epsl.2007.05.046)
197. Herzberg C, Condie K, Korenaga J. 2010 Thermal history of the Earth and its petrological expression. *Earth Planet. Sci. Lett.* **292**, 79–88. (doi:10.1016/j.epsl.2010.01.022)
198. Davies GF. 2009 Effect of plate bending on the Urey ratio and the thermal evolution of the mantle. *Earth Planet. Sci. Lett.* **287**, 513–518. (doi:10.1016/j.epsl.2009.08.038)
199. Ganne J, Feng X. 2017 Primary magmas and mantle temperatures through time. *Geochem. Geophys. Geosyst.* **18**, 872–888. (doi:10.1002/2016GC006787)
200. Zhong S, Zhang N, Li Z-X, Roberts JH. 2007 Supercontinent cycles, true polar wander, and very long-wavelength mantle convection. *Earth Planet. Sci. Lett.* **261**, 551–564. (doi:10.1016/j.epsl.2007.07.049)
201. Rolf T, Coltice N, Tackley PJ. 2012 Linking continental drift, plate tectonics and the thermal state of the Earth's mantle. *Earth Planet. Sci. Lett.* **351–352**, 134–146. (doi:10.1016/j.epsl.2012.07.011)
202. Bunge H-P, Richards MA, Baumgardner JR. 1996 Effect of depth-dependent viscosity on the planform of mantle convection. *Nature* **379**, 436. (doi:10.1038/379436a0)
203. Grigné C, Labrosse S, Tackley PJ. 2005 Convective heat transfer as a function of wavelength: Implications for the cooling of the Earth. *J. Geophys. Res. Solid Earth* **110**. (doi:10.1029/2004JB003376)
204. Moore WB, Webb AAG. 2013 Heat-pipe Earth. *Nature* **501**, 501–505. (doi:10.1038/nature12473)
205. Rozel AB, Golabek GJ, Jain C, Tackley PJ, Gerya T. 2017 Continental crust formation on early Earth controlled by intrusive magmatism. *Nature* **545**, 332–335. (doi:10.1038/nature22042)
206. Fischer R, Gerya T. 2016 Early Earth plume-lid tectonics: a high-resolution 3D numerical modelling approach. *J. Geodyn.* **100**, 198–214. (doi:10.1016/j.jog.2016.03.004)
207. Belousova EA, Kostitsyn YA, Griffin WL, Begg GC, O'Reilly SY, Pearson NJ. 2010 The growth of the continental crust: constraints from zircon Hf-isotope data. *Lithos* **119**, 457–466. (doi:10.1016/j.lithos.2010.07.024)
208. Gurnis M. 1988 Large-scale mantle convection and the aggregation and dispersal of supercontinents. *Nature* **332**, 695–699. (doi:10.1038/332695a0)
209. Lenardic A, Moresi LN, Jellinek AM, Manga M. 2005 Continental insulation, mantle cooling, and the surface area of oceans and continents. *Earth Planet. Sci. Lett.* **234**, 317–333. (doi:10.1016/j.epsl.2005.01.038)
210. Rolf T, Tackley PJ. 2011 Focussing of stress by continents in 3D spherical mantle convection with self-consistent plate tectonics. *Geophys. Res. Lett.* **38**. (doi:10.1029/2011GL048677)
211. Rey PF, Coltice N, Flament N. 2014 Spreading continents kick-started plate tectonics. *Nature* **513**, 405–408. (doi:10.1038/nature13728)
212. Moyen J-F, van Hunen J. 2012 Short-term episodicity of Archaean plate tectonics. *Geology* **40**, 451–454. (doi:10.1130/g322894.1)
213. O'Neill C, Marchi S, Zhang S, Bottke W. 2017 Impact-driven subduction on the Hadean Earth. *Nat. Geosci.* **10**, 793–797. (doi:10.1038/ngeo3029)
214. Hansen VL. 2007 Subduction origin on early Earth: a hypothesis. *Geology* **35**, 1059–1062. (doi:10.1130/G24202A.1)

215. Gerya TV, Stern RJ, Baes M, Sobolev SV, Whattam SA. 2015 Plate tectonics on the Earth triggered by plume-induced subduction initiation. *Nature* **527**, 221–225. (doi:10.1038/nature15752)
216. Furnes H, de Wit M, Dilek Y. 2014 Four billion years of ophiolites reveal secular trends in oceanic crust formation. *Geosci. Front.* **5**, 571–603. (doi:10.1016/j.gsf.2014.02.002)
217. Furnes H, Dilek Y. 2017 Geochemical characterization and petrogenesis of intermediate to silicic rocks in ophiolites: a global synthesis. *Earth Sci. Rev.* **166**, 1–37. (doi:10.1016/j.earscirev.2017.01.001)
218. Kamber BS. 2015 The evolving nature of terrestrial crust from the Hadean, through the Archaean, into the Proterozoic. *Precambrian Res.* **258**, 48–82. (doi:10.1016/j.precamres.2014.12.007)
219. van Hunen J, Moyen J-F. 2012 Archean subduction: fact or fiction? *Ann. Rev. Earth Planet. Sci.* **40**, 195–219. (doi:10.1146/annurev-earth-042711–105255)
220. Domeier M, Torsvik TH. 2017 Full-plate modelling in pre-Jurassic time. *Geol. Mag.* (doi:10.1017/S0016756817001005)
221. Domeier M, Torsvik TH. 2014 Plate tectonics in the late Paleozoic. *Geosci. Front.* **5**, 303–350. (doi:10.1016/j.gsf.2014.01.002)
222. Matthews KJ, Maloney KT, Zahirovic S, Williams SE, Seton M, Müller RD. 2016 Global plate boundary evolution and kinematics since the late Paleozoic. *Global Planet. Change* **146**, 226–250. (doi:10.1016/j.gloplacha.2016.10.002)
223. Merdith AS *et al.* 2017 A full-plate global reconstruction of the Neoproterozoic. *Gondwana Res.* **50**, 84–134. (doi:10.1016/j.gr.2017.04.001)
224. Popper K. 1959 *The Logic of Scientific Discovery*. London, UK: Routledge Classics.